4-13-2017 12:00 AM

Assessing the role of Ku70 vWA domain phosphorylation in the inhibition of Aurora B and activation of the DNA damage response

Elizabeth A. Walden, *The University of Western Ontario*

Supervisor: Dr. Caroline Schild-Poulter, *The University of Western Ontario*

A thesis submitted in partial fulfillment of the requirements for the Master of Science degree in Biochemistry

Abstract

Ku is a key component of the Non-Homologous End Joining DNA repair pathway. Recently, a function for Ku in DNA damage response (DDR) signalling was identified through studies exploring a Ku70 S155D phosphomimetic mutant. We hypothesize that Ku70 S155D mimics phosphorylation of Ku70 in response to DNA damage, and that Ku S155 phosphorylation inhibits Aurora B leading to sustained DDR activation. In this study we show that the S155D mutant is competent for heterodimerization, and its expression does not induce DNA damage. Phosphorylated Ku70 associates with Aurora B by co-immunoprecipitation and this association was demonstrated *in situ* with Ku70 S155D. Additionally, we demonstrate that the Ku70 S155D vWA domain is sufficient to inhibit Aurora B in an *in vitro* kinase assay. Finally, Aurora B inhibitor treatment of Ku70 S155D cells does not increase the prevalence of a DDR marker γH2AX. This work suggests that Ku70 S155 phosphorylation inhibits Aurora B which in turn leads to DDR activation.

Keywords: DNA double strand breaks, Non-homologous end joining, DNA damage response, Cell cycle arrest, Ku, Aurora B

Co-Authorship Statement

This thesis was written by Elizabeth Walden and reviewed and edited by Elizabeth Walden and Dr. Caroline Schild-Poulter. Plasmid constructs that were made by Victoria Fell or with the help of Louisa Salemi and are acknowledged as such in the methods section. Some of the work contained in this thesis is published in Scientific Reports: Ku70 serine 155 mediates Aurora B inhibition and activation of the DNA damage response.

Acknowlegements

To begin, I would like to thank my supervisor Dr. Caroline Schild-Poulter for her support and mentorship through the process of my experiments and the writing of this thesis. I would like to thank my committee members, Dr. Brandl, and Dr. Cregan, for their insightful critiques and suggestions that led to success in my work. In addition, thank you to Dr. Cregan and Dr. Poulter for the use of their ChemiDoc and immunofluorescent microscope, respectively. Thank you to Dr. Aaron Goodarzi for his advice on the performance of Comet Assays. Additionally, I am extremely appreciative to have been the recipient of funding for my research in the form of a NSERC Canada Graduate Scholarship- Master's and an Ontario Graduate Scholarship. I would also like to thank my examiners for taking time out of their busy schedules to review my thesis and attend my defence.

In my day to day work, my colleagues in the lab were essential for bouncing problem solving ideas off of, and of course for all the laughs and ongoing support. Therefore I want to thank all past and current members of the of Dr. Schild-Poulter's lab for setting me up for success. Specific thanks to: Louisa Salemi, Xu Wang, Sarah Hoffer, Christina McTavish, Matthew Maitland, Christopher Chiasson, and Sanna Abbasi as well as our many excellent undergraduate students for their friendship and help keeping me positive through the ups and downs. To my boyfriend, Graham: Thank you for your help with everything related to computers and for being a constant supporter of me. Finally, I would like to thank my parents for their support of everything I do. Everything you have done for me has helped me to get to this point and thank you for supporting me to continue on to my Ph.D. research.

Contents

List of Figures

List of Tables

Acronyms

γH2AX Phosphorylated H2AX.

53BP1 p53 binding protein 1.

aNHEJ alternative Non-Homologous End Joining.

ATF2 activating transcription factor 2.

ATM ataxia telangiectasia mutated.

ATR ataxia telangiectasia and Rad3 related.

Bax Bcl-2 associated X.

CCS Canadian Cancer Society.

CDK cyclin dependent kinase.

CHK1 checkpoint kinase 1.

CHK2 checkpoint kinase 2.

cNHEJ classical Non-Homologous End Joining.

COSMIC Catalogue of Somatic Mutations in Cancer.

CPC chromosomal passenger complex.

CtIP CtBP-interacting protein.

DAPI 4',6-diamidino-2-phenylindole.

DDR DNA Damage Response.

DMEM Dulbecco's Modified Eagle's Medium.

DMSO Dimethyl sulfoxide.

DNA-PK DNA-dependent protein kinase.

DNA-PKcs DNA-dependent protein kinase catalytic subunit.

DSBR double strand break repair.

DSBs double strand breaks.

FBS fetal bovine serum.

FITC fluorescein isothiocyanate.

FL full length.

H_2O_2 hydrogen peroxide.

HEPES Hydroxymethyl piperazineethanesulfonic acid.

HPA1α Heterochromatin Protein 1.

INHAT inhibitor of histone acetyltransferases.

IP immunoprecipitation.

IPTG Isopropyl β-D-1-thiogalactopyranoside.

IR irradiation.

Ku70$^{-/-}$, KO knockout.

LB Lysogeny broth.

Mcl-1 induced myeloid leukemia cell differentiation protein.

MDM2 mouse double minute 2 homolog.

MMEJ microhomology-mediated end joining.

MRN Mre11, Rad50, and Nbs1.

Nbs1 Nibrin.

PARP1 Poly [ADP-ribose] polymerase 1.

PBS phosphate buffered saline.

PIKK phosphoinositide three-kinase-related kinase.

PLA Proximity ligation assay.

PNKP polynucleotide kinase/phosphatase.

PP1 Protein phosphatase 1.

PUMA p53 upregulated modulator of apoptosis.

PVDF polyvinylidine difluoride.

RAG recombination activating gene.

Rb Retinoblastoma protein.

RPA replication protein A.

SDS-PAGE sodium dodecyl sulfate polyacrylamide gel electrophoresis.

SDSA synthesis-dependent strand annealing.

SEM standard error of the mean.

TBS-T Tris buffered saline-Tween-20.

Tet-Off Tetracycline-repressible.

V(D)J Variable, Diversity and Joining.

vWA von Willebrand A.

WIP1 wild-type p53-induced phosphatase 1.

WT wild-type.

XLF XRCC4-like factor.

XRCC4 X-ray Repair Cross-Complementing protein 4.

YY1 Yin Yang 1.

Chapter 1

Introduction

This section summarizes the prevalence of, and previous research on DNA breaks, with a specific focus on double stranded DNA breaks, their repair, and the DNA damage response. In addition, it introduces previous work in the field which, in turn, forms the background for the hypothesis and objectives.

1.1 Cancer

When it comes to research regarding human disease, understanding cancer is critically important. While all cancers are labelled under one broad umbrella, the different tissues of origin and mutations leading to tumourogenesis and metastasis make this group of diseases extremely complex, with each case arising in a slightly different manner. The Canadian Cancer Society (CCS) projected that in 2016, over 200 000 people would be diagnosed with cancer, an average of approximately 555 people per day [1]. The CCS also states that 2 in 5 Canadians are expected to develop cancer over the course of their lives, and 1 in 4 are expected to die from the disease [1]. While these statistics are concerning, the body of research investigating cancer is considerable and there have been immense advancements in survival rates over recent decades [1].

While cancer is a set of over 200 distinct diseases there are commonalities between them. Hanahan and Weinberg, coined six hallmarks of cancer which have been generally accepted by the field: evading apoptosis, self-sufficiency in growth signals, insensitivity to anti-growth

signals, sustained angiogenesis, limitless replicative potential, and tissue invasion and metastasis [2]. A subsequent revision of these hallmarks identified genomic instability as the most prominent tumorogenesis enabling characteristic [3]. Genome instability is a characteristic of cancer cells but also represents a therapeutic target. Ionizing radiation and chemotherapeutic drugs are commonly used to kill cancer cells. These treatments induce DNA breaks which are repaired by healthy cells while being toxic to the rapidly dividing tumour cells. Overall, the study of deregulated proliferation, genome instability, and the associated exploitation of this genome instability are major fields within cancer research.

1.2 Double stranded DNA breaks

DNA carries the genetic information for a cell and is therefore vital to each cell's survival and proper function. There are many types of DNA damage, but DNA double strand breaks (DSBs) are one of the most disruptive and dangerous. DNA DSBs are a threat to the continuity and integrity of DNA [4]. They are a physical break in both strands of the DNA, which means that if left unrepaired, genetic infomation could be lost following cell division [4]. Additionally, the incorrect repair of DNA lesions has the potential to be dangerous through recombination and the associated generation of novel sequences [4]. These disruptions to the genome can lead to the development of oncogenic properties [4]. Given how dangerous these DNA breaks can be to a cell they are surprisingly common and can be created by either endogenous or exogenous sources including: ionizing radiation, chemotheraputic agents, free radicals, and reactive oxygen species [5]. Additonally, there are cell specific processes that create DSBs to induce diversity in the immune system such as Variable, Diversity and Joining (V(D)J) recombination and immunoglobulin class switch recombination [6]. Interestingly, Ciccia and Elledge estimated the number of DSBs created per cell by some common activities including: a body CT scan at 0.28 DSBs/cell, a 5 hour flight at 0.001 DSBs/cell, a 60 day space mission at 2 DSBs/cell, and external beam therapy (1,800 to 2,000 mSv dose) at 80 DSBs/cell [7]. A separate group estimated that 50 DSBs may arise per cell cycle, primarily created due to reactive oxygen species [8]. Based on these estimates and taking into consideration the huge number of cells in the human body it is clear that efficient DNA double strand break repair pathways are required for survival.

1.3 Double stranded DNA break repair

The repair of damaged DNA is necessary to prevent loss of genetic information, misrepair causing sequence alterations, or possible neoplastic transformations [9]. The importance of DNA DSB repair is underlined by the fact that eukaryotic cells have developed three different pathways to repair DNA DSBs [4]. These pathways are: Homologous Recombination, classical Non-Homologous End Joining, and alternate Non-Homologous End Joining. Each of these have a specific role in the cell and while these pathways are mechanistically different, they converge to ensure the repair of DNA double strand breaks [4]. The decision of which pathway acts to repair a DSB is dependent on both the cell cycle stage of the cell and the type of ends produced in the DSB [10]. These repair pathways are frequently deregulated in cancer [11, 12, 13].

1.3.1 Homologous recombination

Homologous recombination requires a homologous sequence in order to repair the DNA break [4, 14]. Therefore, this repair pathway is most efficient when the cell is in either the S or G2 phase of the cell cycle, as following DNA synthesis there are two copies of each chromosome [4, 14, 15]. The template-dependent repair by homologous recombination means that it has high fidelity and a much lower error rate than other repair pathways [14].

There are two models for this pathway: double strand break repair (DSBR) and the second is synthesis-dependent strand annealing (SDSA). Both models begin with the generation of 3' single strand overhangs through strand resection by nucleases such as Mre11 and CtBP-interacting protein (CtIP) [14, 16]. The subsequent binding of RAD51 to the ssDNA end creates a nucleoprotein filament capable of invading into the double stranded chromosome that is the complementary to the damaged DNA [14]. The homologous DNA is then used as a template to repair the damaged strand [10]. Here the two models diverge. In DSBR, the second end of the DSB is captured by the D-loop created during synthesis and two Holliday junctions (cross shaped structures of 4 DNA strands) are produced [17]. The resolution of these junctions can result in crossover or non-crossover products, and is therefore associated with meiotic recombination [17]. In SDSA, the D loop does not capture the second end of the break. Instead the newly formed DNA dissociates from the template and is able to bind to the non invading broken DNA end [17]. In both cases the repaired strand is identical in sequence to the template sister chromatid, making this repair less error prone than other repair pathways.

1.3.2 Classical Non-Homologous End Joining

In the G0/G1 stage of the cell cycle the DNA has not been replicated, therefore template-independent repair pathways have also evolved in eukaryotes [4, 14, 15]. One fast, but slightly error prone pathway, is the classical Non-Homologous End Joining (cNHEJ) pathway which can function throughout the cell cycle but is primarily restricted to the G0/G1 and early S stages [10, 18]. As mammalian cells spend most of their time in the G0/G1 stage of the cell cycle this is the primary DNA DSB repair pathway of mammalian cells, and is therefore vital in maintaining regulation of genomic stability [6]. The cNHEJ pathway is central in this work specifically.

The cNHEJ acts by ligating the two ends created in an DSB back together, and this process is oulined in Figure 1.1. The repair of DSBs by cNHEJ is initiated when the Ku heterodimer (Ku70 and Ku80), the primary DNA binding component of this pathway, encircles the ends of the DNA break [19]. Following this initial recognition of the break, the Ku heterodimer recruits the DNA-dependent protein kinase catalytic subunit (DNA-PKcs) and translocates along the DNA by 1 helical turn [4, 10]. This creates the fully functional DNA-dependent protein kinase (DNA-PK) complex, composed of Ku and DNA-PKcs. This complex then phosphorylates a number of targets including Ku, Artemis, X-ray Repair Cross-Complementing protein 4 (XRCC4), ligase IV, XRCC4-like factor (XLF), and other molecules of DNA-PK [4, 6]. The phosphorylation and recruitment of these proteins, as well as the recruitment of DNA polymerases, creates a DNA-protein complex with the two ends stabilized and tethered together using filaments made of XLF-XRCC4 [20].

Ligation can only occur between blunt DNA ends with 5'phosphates and 3'hydroxyl groups. In order to process more complex ends, Artemis exhibits endonuclease activity to open hairpin structures as well as processing of complex DNA ends [4, 21, 22]. Additionally Ku and an XRCC4-polynucleotide kinase/phosphatase (PNKP) complex have each been demonstrated to have end processing activity [23, 24]. At this point, the two blunt ends of the DNA are held in proximity to each other for ligation by the XRCC4-Ligase IV-XLF complex. This complex ligates across the break restoring the single continuous strand of double stranded DNA [4]. Finally, following repair, the stable Ku heterodimer must be removed from the DNA. Since the two subunits of Ku are intertwined, they cannot be removed by conformational change alone. It is therefore proposed that the removal occurs through the polyubiquitylation of Ku80 and a ubiquitin-dependent protein degradation [25, 26].

Classical Non-Homologous End Joining is not only responsible for the repair of DNA double strand breaks that occur accidentally but also for those generated by cell-specific recombination activating gene (RAG) proteins in the immune system [27]. This cleavage by RAG proteins, which occurs during lymphocyte differentiation, creates fragments containing variable (V), joining (J), and diversity (D) gene segments which can then be rearranged and ligated together through the cNHEJ pathway [27]. The cNHEJ pathway is essential in V(D)J recombination in the creation of antigen receptor genes [4]. This process is required for creating a diverse set of antigen binding sites for the receptors [4]. In addition, the repair of DSBs in immunoglobulin class switch recombination allows for the production of distinct antibodies [4]. The deletions and insertion errors associated with cNHEJ are an advantage in these processes, as they create diversity in sequences [4]. This role of the cNHEJ in the production of T-cell receptors and immunoglobulins underlies the immunodeficiency seen in patients deficient for members of the cNHEJ pathway [28, 29, 30].

1.3.3 Alternate Non-Homologous End Joining

Accompanying the two well-characterized pathway previously discussed, there exists a collection of pathways that act as backup systems of DSB repair which are independent of key proteins involved in cNHEJ and HR repair [32]. These alternate pathways have been termed alternative Non-Homologous End Joining (aNHEJ), B (backup)-NHEJ, or microhomology-mediated end joining (MMEJ) [32, 33]. As these names imply, this repair mechanism does not rely on a template for the repair process but works through the alignment of microhomolgies, short regions of DNA complementarity, on opposite ends allowing for ligation of the broken ends [32]. Relatively little is known about this collection of pathways but they appear to be backup repair pathways that can initiate DSB repair in cells deficient in cNHEJ capabilities [4]. However, this set of pathways is also functional in cells that are proficient for cNHEJ [4]. Although much remains to be characterized about this set of repair pathways, several key factors including Poly [ADP-ribose] polymerase 1 (PARP1), CtIP, ataxia telangiectasia mutated (ATM), and the Mre11, Rad50, and Nbs1 (MRN) complex are thought to facilitate the repair [34]. There is evidence that PARP1 acts as the initial DNA break sensing factor, as well as tethering the ends and recruiting factors for repair [32]. The recruitment of these factors likely leads to end resection and the exposure of microhomologies at DNA ends which can subsequently be used to ligate and repair the DNA [32]. Ligase 3 in mammalian cells has been suggested to play a role in aNHEJ [32]. aNHEJ repair of DNA DSBs is effective but highly error prone, commonly leading to chromosome translocations [4, 35].

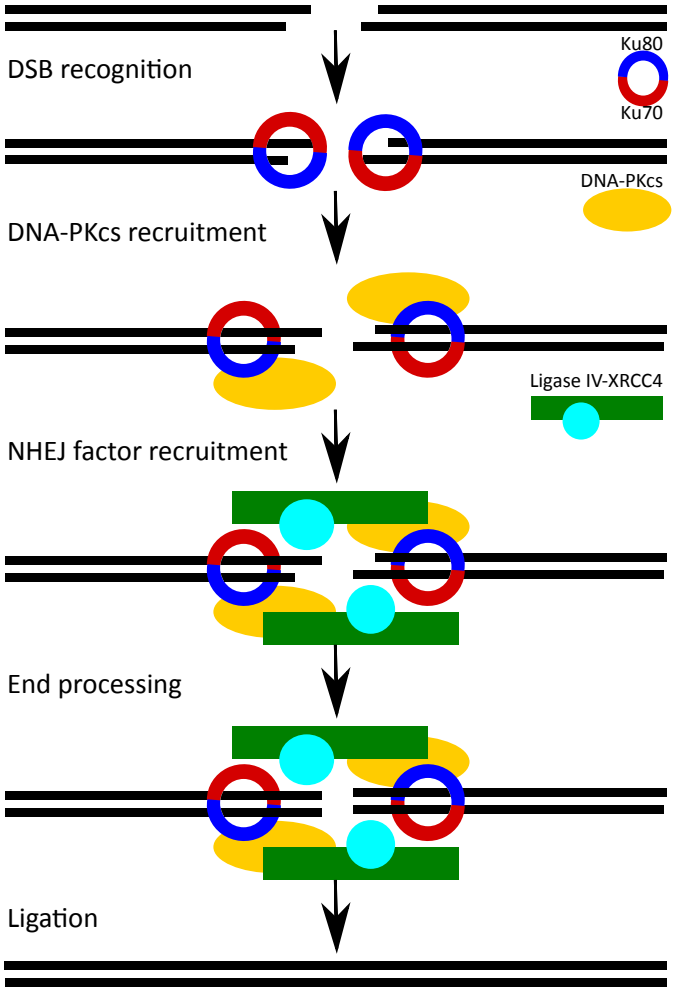

Figure 1.1: Overview of the classical Non-Homologous End Joining pathway. Upon induction of a DNA DSB, the break is recognized by the Ku70/Ku80 heterodimer. The subsequent recruitment of DNA-PKcs completes DNA-PK at the break and leads to the recuitment of other cNHEJ factors including Ligase IV and XRCC4. Additonally, in order to process ends: Artemis, PNKP, and DNA polymerases are recruited. This leads to end joining and the dissociation and removal of the cNHEJ factors. The result is one continuous length of double stranded DNA. This schematic is derived from Dueva and Iliakis, 2013 [31].

1.3.4 DNA DSB repair pathway choice

These three classes of DNA DSB repair co-exist in each cell, therefore upon induction of a DSB a cell must "choose" which mechanism will repair the break [4, 36, 37]. This pathway choice is regulated and there exists competition between pathways [4]. There are a number of factors that influence this pathway repair. The binding of Ku is a key modulator of choice which favours cNHEJ by suppressing aNHEJ and preventing end resection which would initiate HR [38]. Additionally, p53 binding protein 1 (53BP1) and associated effector genes promote cNHEJ by restricting end resection [36, 37]. Conversely, proteins including CtIP and Mre11 promote end resection and therefore HR repair [36]. It has also been demonstrated that the histone code, specifically pre-existing chromatin structures at the break, may influence pathway choice at that location [36]. Much of this pathway competition is decided by which proteins bind first and are therefore able to out compete and repress the other pathways. Additionally, the antagonization of Ku70 binding by end resection is also a key step in pathway choice [39]. However, it has also been demonstrated that in some cases bound Ku and MRN are removed from complex DSBs in a CtIP and Mre11 dependent manner allowing for repair by HR [40]. The complex interplay of proteins in pathway choice is also dependent on the presence of a sister chromatid to the broken DNA, and is therefore cell cycle stage dependent [4]. Overall, the regulation of pathway choice is vital in fast and efficient repair of DSBs.

1.4 DNA damage response

In addition to initiating the repair of a double stranded DNA break following DNA damage, the cell mounts a DNA Damage Response (DDR) [41]. This DDR occurs in parallel with, and in some cases is required for, DNA repair and signals to inhibit cyclin-cyclin dependent kinase (CDK) complexes from promoting cell cycle progression, thereby arresting the cells at the G1/S, S, and G2/M cell cycle checkpoints [42, 43]. This cell cycle arrest prevents DNA replication and mitosis from occurring in the presence of DNA breaks [41]. This process acts as a safeguard to preserve genetic integrity and in this role also acts to prevent neoplastic transformation of cells [10]. Additionally, in the case of overwhelming damage, this pathway will also stimulate senescence or apoptosis in the damaged cell [44, 45]. The overarching goal of the DDR is to protect the cell and in the case that DNA cannot be repaired prevent the threat of cellular deregulation to the organism [7]. This pathway is outlined below and in Figure 1.2.

The DDR is a highly controlled signalling network which has evolved to function primarily through quick changes in post-translational modifications and transcriptional changes [46]. The initial post-translational modifications in the DDR are primarily phosphorylation and dephosphorylation events which allow for specific activation and inactivation of members of the network [7, 46]. The master kinases responsible for initiation of the DDR are members of the phosphoinositide three-kinase-related kinase (PIKK) family [10]. Specifically, ATM and ataxia telangiectasia and Rad3 related (ATR) kinases are the master controllers of the DDR, with much of the signalling cascade being regulated by phosphorylation states of the pathway members [10]. A proteomic study by Matsuoka and colleagues assessed proteins phosphorylated at ATM and ATR consensus sequences (SQ/TQ) following induction of DNA damage and identified over 900 phosphorylation sites on over 700 proteins [47]. This demonstrates the vast network of proteins and phosphorylation events involved in this pathway [47]. The ATR-dependent signalling pathway is stimulated in response to the recruitment of replication protein A (RPA) to a single strand in end resection or at stalled replication forks, while the ATM-dependent pathway is initiated by the inital MRN recruitment to DNA double strand breaks following a DNA-damaging agent induction of a DNA break [7, 10, 46]. However, these pathways are heavily intertwined as they involve many of the same transducers and downstream targets [46].

The ATM-dependent pathway will be of focus in this work as it is the pathway that functions primarily in the repair of DSBs, however it is interesting to note that ATM-dependent activation of ATR signalling has also been documented [46, 48]. The ATM-dependent DDR signalling cascade begins with the recruitment of the MRN complex to a DSB [44]. This complex is necessary for the recruitment, autophosphorylation, and subsequent activation of ATM [42]. The autophosphorylation of ATM at serine 1981 is associated with it dissociating from an inactive dimer into two active monomer particles [10]. This in turn leads to ATM phosphorylating a number of mediators and downstream kinases including 53BP1, histone H2AX, Nibrin (Nbs1), checkpoint kinase 1 (CHK1), and checkpoint kinase 2 (CHK2) [10, 49]. The MRN complex is both a sensor for DNA damage and tethers DNA ends together [10]. Specifically, the C-terminus of Nbs1 within the MRN complex is responsible for the recruitment of ATM to DNA DSBs leading to ATM activation [50]. The recruitment of ATM to DNA is necessary for its activation and function in phosphorylating CHK2 and other factors which are localized to sites of DNA damage [50].

Phosphorylated ATM and CHK2 lead to phosphorylation, stabilization, and upregulation of p53 [42]. p53 is a key transducer within this pathway and regulates the levels of many other

proteins through transcriptional activation. This includes p21, a cyclin-CDK inhibitor, as well as pro-apoptotic factors Bcl-2 associated X (Bax) and p53 upregulated modulator of apoptosis (PUMA) [7, 51]. p21 inhibits CyclinD/CDK4/6 and CyclinE/CDK2 complexes therefore blocking the cell cycle from progressing. Additionally, the upregulation of p53 leads to the upregulation of wild-type p53-induced phosphatase 1 (WIP1) and mouse double minute 2 homolog (MDM2) protein phosphatases which perform a negative feedback function through inhibiting ATM and p53 [52]. This creates a cyclical oscillation in p53 which maintains the cell cycle arrest, but likely also acts as a measurement of persistent DNA damage and signalling for apoptosis [52]. Therefore, this pathway initially gives the cell time to repair damage before mitosis through p21 dependent cell cycle arrest but in the event that the DNA is not repaired, p53 persistent oscillation may lead to activation of apoptosis. The activation of caspases and apoptosis occurs through p53-dependent activation of apoptotic factors Bax and PUMA and is necessary to kill off cells that are unable to repair their DNA and return to a normal state [52].

Other factors, such as H2AX, that are phosphorylated by ATM are important for the recruitment of DDR proteins to the break site and the associated cascade of protein modifications [7]. H2AX is a histone variant which is incorporated into histone octamers [44]. Phosphorylated H2AX (γH2AX) is the most prominent modification in DDR and occurs over several megabases around DSBs which in turn serves as a docking site for other members of the DDR pathway [44]. Additionally, downstream targets, specifically γH2AX and 53BP1, form foci at breaks and therefore are markers for DNA damage that can be identified using immunofluorescence assay [19, 44].

While the role of kinases in the DDR is well characterized, the dephosphorylation of proteins by phosphatases in the DDR pathway is additonally of interest [46, 53]. Protein phosphatase 1 (PP1) is one of the most studied phosphatases in the DDR, as well as being one of the most abundant [53]. PP1 has been demonstrated to regulate the DDR, specifically by supressing its activation and creating a threshold for DNA damage necessary to induce a DDR [54]. The protein Repo-Man (recruits PP1 onto mitotic chromatin at anaphase) is a target of CDK1 phosphorylation downstream of ATM and as its name mentions, is responsible for recruiting PP1 to DNA [54]. The recruitment of PP1 to DNA prevents activation of the DDR through the modulation of ATM activity by dephosphorylating the Ser 1981 site [54]. ATM and PP1 bind to different areas on the Repo-Man molecule. Therefore, it is speculated that Repo-Man-dependent proximity of PP1 and ATM allows for the dephosphorylation of ATM and the suppression of the DDR [54]. Based on this work, dephosphorylation, in opposition to phosphorylation, aids in the regulation and threshold determination of the DDR. However, the

phosphorylation of I-2 (an inhibitor of PP1) by ATM leads to its dissociation from PP1, activating PP1. This in turn inhibits another kinase, Aurora B, which will be described later [55]. In this example, PP1 is activated in response to DDR, supporting that the role of phosphatases in the DDR is more complex than a simple role in maintaining a threshold for activation.

In addition to phosphorylation and dephosphorylation, many other post translational modification have been identified to occur at sites of DNA damage and in the DDR. Briefly, ubiquitination, methylation and acetylation of histones, and sumoylation of proteins such as XRCC4 and Ku at the break have been identified as a few of the likely many other types of post translational modifications that also play a role in modulation of the DDR [43].

The complex network of interactions in the DDR lead overall to 2 outcomes: If the DNA is repaired the cell can resume normal cell cycling. Otherwise, the cell activates apoptosis to destroy the cell and protect the organism as a whole [41, 46]. As an alternative to apoptosis, the cell can enter senescence, which functionally also removes the threat of the unrepaired break by preventing the cell from replicating [45].

1.5 Ku

Ku acts as the initial binding component of the cNHEJ DNA repair pathway and leads to the recruitment of factors required to repair the DSB [4]. Ku is a heterodimer that consists of a Ku70 and a Ku80 subunit. The Ku proteins are conserved throughout eukaryotes and more recently homologues have been identified in Archaea and Bacteria [56]. Ku is extremely abundant in human cells with estimates at 400 000 molecules per cell and it binds strongly to DNA DSBs [27]. Ku70 and Ku80 exist in cells as a heterodimer and heterodimerization appears to be required for the stability of each individual monomer [56]. This is demonstrated by the severely reduced levels of Ku70 in Ku80 knockout cells and *visa versa* [56]. The importance of Ku70 and the cNHEJ is demonstrated in Ku70 knockout mice. These mice are viable and fertile but are immunodeficient, exhibit premature aging, and are approximately 50% of the size of control mice [57, 58]. In addition, Ku70-deficient mice have an increased prevalence of thymic tumour formation [57]. Finally, cells that are deficient in Ku70 or Ku80 are extremely radiation sensitive [15].

Ku70 (XRCC6) and Ku80 (XRCC5) were initially identified as targets of autoantibodies in a patient diagnosed with scleroderma polymitosis overlap syndrome [33]. This pair of pro-

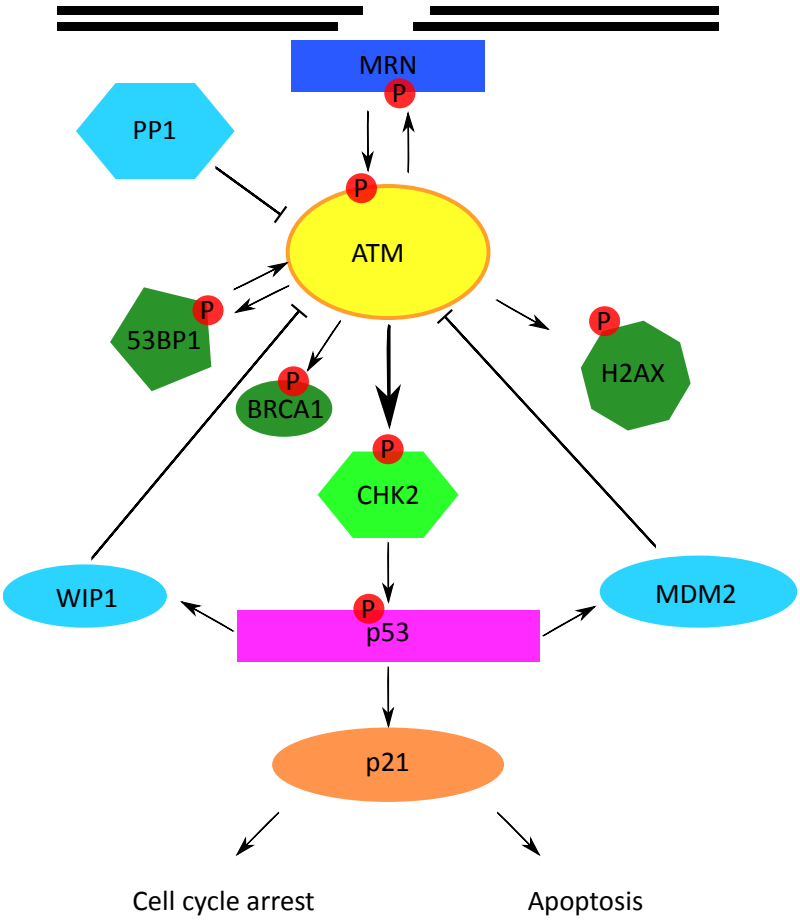

Figure 1.2: Overview of the DNA damage response pathway. Upon induction of a DSB by endogenous or exogenous factors the MRN complex acts as a DNA damage sensor. The recuitment of the MRN complex leads to the autophosphorylation and activation of ATM, the apex kinase in this pathway. ATM then phosphorylates mediators of the DDR including CHK2. CHK2 then leads to p53 phosphorylation and activation which in turn induces p21. p21 causes cell cycle checkpoint arrest or in states of overwhelming or unrepaired damage, apoptosis activation. Additionally this schematic includes number of downstream markers for DDR activation such as 53BP1, γH2AX, and p21. Only some of the major components of this pathway are shown. This schematic was derived from Sulli *et. al.*, 2012 [49].

teins were named based on the patient's initials (K.U.) and their SDS-PAGE mobilities [27]. The proteins were subsequently identified as nuclear proteins with DNA binding capabilities, specifically in a sequence independent manner for DNA discontinuities [33, 59, 60]. Subsequently, the Ku subunits were identified as acting in DNA repair, specifically playing a role in the cNHEJ [4, 10, 33]. While Ku70 and Ku80 are divergent in sequence they are quite similar in structure and they function as a heterodimer [33].

1.5.1 Ku70 structure

Ku70 is a 70 kDa protein that is composed of 3 major domains: a core DNA binding domain, a helical C-terminal domain, and a N-terminal von Willebrand A (vWA) like α-β domain (Figure 1.3) [61, 62]. The core domain is responsible for the heterodimerization of Ku70 with Ku80 [33]. Additionally, the formation of the heterodimer, through the core domains, creates a ring structure lined with positive charges which bind DNA breaks in a sequence independent manner [33]. The C-terminal domain of Ku70 is the most divergent region from Ku80 in structure [33]. The C-terminal of Ku70 is much smaller than that of Ku80 and consists of a SAP domain (SAF-A/B, Acinus, and PIAS motifs) which is linked to the rest of the protein through a linker region [63]. The deletion of C-terminal domain decreases DNA DSB binding of Ku suggesting that it is involved in DNA interaction [63]. The N-terminal vWA like domain is composed of a Rossmann fold type six-stranded β-sheet with one antiparallel strand [61]. The amino end of the vWA domain is in contact with the bound DNA while the carboxyl end faces away from the DNA [61]. This means that the outer side of the vWA domain protrudes from the complex formed at a DNA DSB where it could be involved in protein-protein interactions [33]. Many characterized vWA domains are found within proteins of the extracellular matrix as well as being involved in cell adhesions [64]. In these roles, the vWA is frequently involved in protein-protein interactions [64]. However, interestingly, very few protein interactions have been mapped to this region of Ku70 [33].

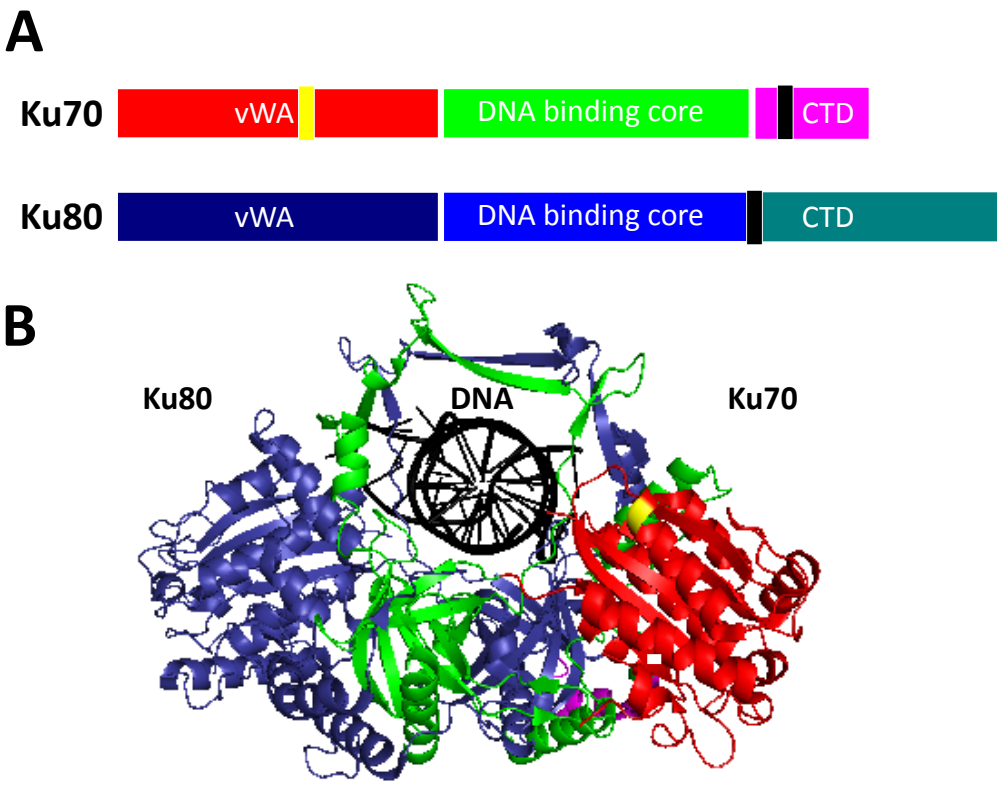

Figure 1.3: Domains and structure of Ku70 and Ku80. A) Schematic of the domains of Ku70 and Ku80. There are three main domains in each: the N-terminal vWA domain (in Ku70 the S155 site is highlighted in yellow), the core DNA binding domain, and the divergent C-terminal domain. The black bar in each denotes the location of the nuclear localization signal. B) The crystal structure of the Ku heterodimer creating an asymetric ring encircing the bound double stranded DNA. The specific domains of Ku70 are colour coded to the schematic in A and the S155 site is highlighted in yellow. The Ku70 and Ku80 C-terminal domains are partially unstructured and therefore are not fully present in the diagram. Structure was obtained from PDB:1JEY [61].

1.5.2 Functions for Ku outside the cNHEJ

In addition to its roles in cNHEJ and the associated V(D)J pathway, Ku70 and Ku80 have been demonstrated to play roles in other cellular processes [33, 56].

Ku proteins have been implicated in the movement of mobile genetic elements [56]. The integration of transposons, retrotransposons, and retroviruses, or their products, into the host genome occurs in a similar fashion to V(D)J recombination [56]. Ku has been demonstrated to facilitate integration of the Ty1 retrotransposon in *S. cerevisiae* [65]. Addtitonally, Ku70 has been demonstrated to interact with the viral genome and Early 1 A (E1A) proteins in adenovirus [66]. It is probable that mobile genetic elements have taken advantage of the role of Ku in DNA repair.

Ku has additionally been suggested to have a cytoplasmic function in apoptosis [67, 68]. Ku70 has been demonstrated to be necessary for the deubiquitination of induced myeloid leukemia cell differentiation protein (Mcl-1) at the K48 position [67]. This deubiquitination stabilizes Mcl-1 and leads to the suppression of apoptosis [67]. In a similar role, Ku70 represses apoptosis by sequestering Bax in the cytoplasm [68, 69]. The sequestration of Bax is also associated with Ku70-dependent deubiquitination of Bax [69].

An important role for Ku occurs at telomeres, the DNA-protein structures at the end of each chromosome. While Ku knockouts in mouse models are viable, several studies into the creation of Ku knockout human cell lines have demonstrated lethality [70, 71]. This lethality through induction of apoptosis has been associated with a role for Ku at telomeres [70]. Similar to DSBs, telomeres are an end to the DNA double strand helix. Therefore it might be expected that Ku and other members of DSB repair pathways may bind and function at telomeres. However, the structure of telomeres has evolved to prevent activation of DNA DSB repair pathways, as to not erroneously join them to another chromosome or broken strand of DNA [33]. Contrary to this theory, Ku binds at telomeres and plays an important role in stability [72]. Ku deficient mice and human cells both show altered telomere length and stability [73]. Ku acts to prevent recombination and degradation at telomeres [72, 74]. Ku also plays a role in telomere lengthening, as demonstrated by its involvement in the recruitment of telomerase to telomeres [75]. Finally, a study in fungus, *Ustilago maydis* specifically, concluded that in this organism Ku acts to suppress activation of the DNA damage response at telomeres [76]. In this work, under a repressible expression system, the reduction in Ku expression was associated with cell cycle arrest at the G2 checkpoint due to activation of the DDR in a MRN dependent manner [76].

1.5.3 Post-translational modifications of Ku70

Ku has been shown to be post-translationally modified in a variety of ways to modulate its many characterized functions.

Ku70 is targeted for acetylation at multiple lysine residues [68, 77]. These acetylation events alter the funtion of Ku70 and can dimimish its ability to repair DNA damage [78]. One example of this is the acetylation of Ku70 by the inhibitor of histone acetyltransferases (INHAT) complex leading to Bax-mediated apoptosis, while Ku not acetylated at this position normally sequesters Bax in the cytoplasm [68, 78, 79]. In contrast, Ku acetylation at a different lysine residue leads to a reduction in DSB affinity [77]. Therefore the manipulation of this acetylation site by Histone Deacetylase (HDAC) activity has been suggested to regulate the efficacy of cNHEJ [77]. As such, treatment with an HDAC inhibitor provides a putative cancer treatment in the sensitizing of cells to chemotherapy by reducing Ku functionality in cNHEJ [77].

Another set of Ku70 post-translational modifications that have been identified are involved in the removal of Ku70 from DNA. Ubiquitination of Ku80 disrupts its DNA binding and may play a role in the removal of the heterodimer [25, 26]. Similarly, research by Brown and colleagues has demonstrated a neddylation-dependent ubiquitination of Ku70 [80]. These authors suggest that the result of these two types of post-translational modifications promotes the release of Ku from repaired DSBs, a necessary function to complete cNHEJ [80].

Finally, Ku70 is phosphorylated under specific conditions [81, 82, 83]. Chan and colleagues identified that *in vitro* DNA-PK phosphorylates Ku70 at the serine 6 position, a sequence which is divergent from the SQ/TQ consensus sequence of DNA-PK phopshorylation [83]. The authors demonstrated that this residue is phosphorylated at low levels *in vivo* [84]. However, this serine 6 phosphorylation was not required for cNHEJ repair [83, 84]. An additional study using bacterially expressed Ku70 identified serine 51, a SQ consensus sequence for phosphorylation site, as an additional DNA-PK phosphorylation site [85]. More recently it was shown that Ku70 phosphorylation at five residues in the 305-316 amino acid area led to increased end-resection, a characteristic of HR repair [86]. This result supports that post-translational modification may play a role in DSB repair pathway choice [86]. A similar body of research showed that Ku70 phosphorylation by cyclin-CDK complexes at specific times within the cell cycle interfered with the interaction of Ku with the repair origin. The subsequent dephosphorylation event following mitosis, allows for Ku-DNA DSB binding in G0 and G1, also supporting its role in repair pathway choice [81]. DNA-PK phosphorylation of Ku70 has also

been linked to activation of Bax-mediated apoptosis through altering the interaction of Ku70 and Bax [87]. Research into the identification and characterization of phosphorylation of Ku70 at tyrosine 530 demonstrated that the phosphorylation at this site decreases acetlyation therefore interplaying with the previously described acetylation of Ku70 in regulation of apoptosis [88]. Phosphorylation of Ku has also been demonstrated to be increased in cancer cells [89]. Phosphorylation of Ku70 at the serine-27 and serine-33 positions increased following irradiation treatment [89]. In addition, cells expressing an alanine residue at these positions (which block phosphorylation) showed a slower repair of DNA DSBs by comet assay as well as an altered proliferation before and after irradiation [89]. The authors concluded that higher levels of pKu70 in cancer cells was associated with an increase in DNA repair but with a decrease in accuracy of repair. From this, they proposed that pKu70 may contribute to the resistance of tumours to DNA damage inducing treatments [89].

Overall these studies demonstrated that Ku70 post-translational modifications play a variety of roles in pathway regulation within the cell.

1.5.4 Ku70 vWA domain mutants

The vWA domain of Ku70 was of specific interest in the study from Fell and Schild-Poulter [90], as this family of domains is classically known to be a protein-protein interaction domain but very few Ku70-interacting proteins had been mapped to this domain [19, 56, 68, 90]. Therefore, in an attempt to determine important structural and sequence specific functions of this region the authors created point mutants within the Ku70 vWA domain [90]. Ku70 WT and mutants were expressed in Ku70 knockout MEFs using a retroviral expression system [90]. Unexpectedly, a S155A/D156A double mutant increased cell survival, relative to wild-type (WT), following DNA damage induction by irradiation (IR) [90]. Analysis by pulse field gel electrophoresis and an *in vivo* plasmid repair assay established that this mutation did not affect DNA repair efficiency, therefore suggesting that the increased survival was not repair-dependent. Instead, the authors identified changes in the DDR and defects in the activation of apoptosis [90]. Specifically, differential gene expression of several apoptosis-related, activating transcription factor 2 (ATF2)-regulated genes was identified. Futher, Ku70 was demonstrated to repress ATF2 activation, and this repression was enhanced in Ku70 S155A/D156A expressing cells [90]. Finally, a S155A Ku70 mutant was sufficient for survival following IR, and a Ku70 S155D phosphomimetic Ku70 reversed this effect. Therefore, the authors implicated the Ku S155 site in the activation of apoptosis through its phosphorylation [90].

1.6 Ku70 S155

This work suggested an important role for Ku70 S155 in DNA damage signalling and the activation of apoptosis. The mutation of the serine to an alanine at the 155 site represents a loss of the OH functional group (Figure 1.4). The OH group on serine side chains are a common site for phosphorylation as a regulator of signalling. Upon mutation to an alanine the site can not be phosphorylated, which Fell and Schild-Poulter proposed could explain the effects of the S155A mutant following irradiation [91]. The authors therefore created a phosphomimetic mutation of the serine to an aspartic acid, Ku70 S155D (Figure 1.4). The expression of the Ku70 S155D mutant in Ku70$^{-/-}$ MEFs increased cell senstivity to DNA damage [90]. Specifically, these cells were hypersensitive to IR to an even greater extent than Ku70-deficient cells. This data is consistent with the S155 site being a site of phosphorylation in response to DNA damage which regulates apoptotic pathways [90].

Fell and colleagues later went on to use mass spectrometry to demonstrate that Ku70 S155 position is phosphorylated in response to IR [91]. Through continued work with the S155A and S155D Ku70 mutants, the authors discovered that the Ku70 S155A expressing MEFs have a slight increase in proliferation relative to WT. Conversely, Ku70 S155D confers a pronounced growth defect relative to WT and this was associated with the induction of cell cycle arrest at the G1/S and G2/M cell cycle checkpoints (Figure 1.5) [91]. The activation of cell cycle checkpoints was also supported by the differential gene expression stimulated by Ku70 S155D expression. Specifically, expression of genes that promote transition through the checkpoints, including Cyclin D, CDK 6, and Cyclin B, were downregulated. In addition, the Ku70 S155 position was demonstrated to regulate ATM activation, induction of p21, and appearance of γH2AX and 53BP1 foci [91]. In WT cells, upon irradiation, ATM was phosphorylated and activated, p21 was induced, and γH2AX and 53bp1 foci were present. However, in Ku70 S155A expressing MEFs these outcomes were dampened. Conversely, Ku70 S155D MEFs showed constitutive ATM activation, p21 expression, and the presence of DDR markers γH2AX and 53BP1 foci, under normal culturing conditions (i.e. without IR treatment or other exogenous sources of DNA damage) [91]. The authors also demonstrated that Ku-DNA binding was not necessary for the induction of DNA damage markers and cell cycle arrest. The Ku70 S155D vWA domain is sufficient to induce this response, in both a Ku null and WT Ku background. Therefore, exogenous Ku70 S155D vWA domain is dominant over endogenous Ku70 in this pathway. Taken together, Ku70 S155D, which mimics Ku70 phosphorylation following DNA damage, activates ATM and a DNA damage response [91].

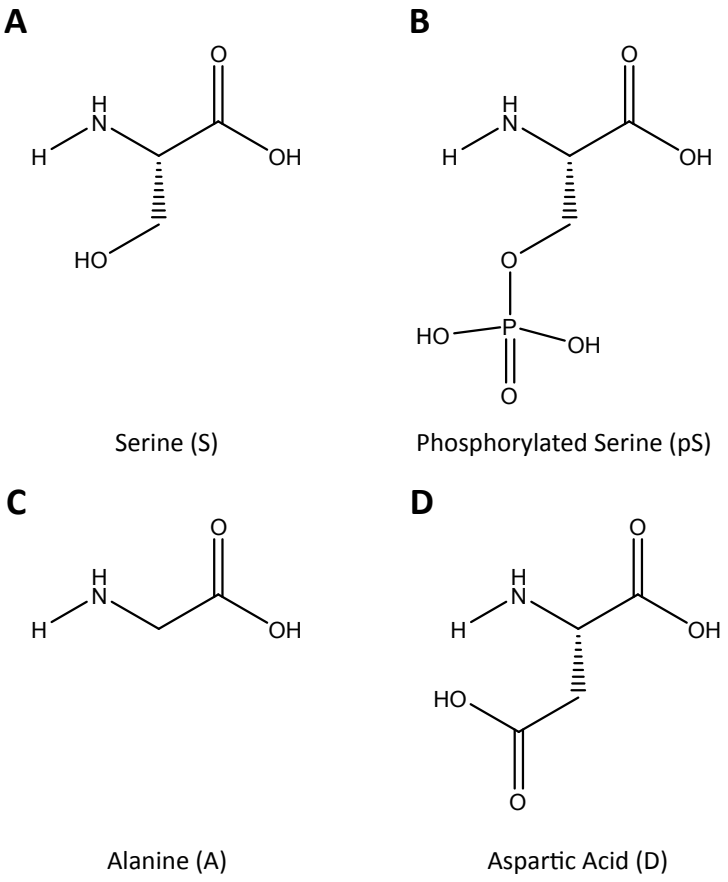

Figure 1.4: Structure of Alanine, Aspartic Acid, Serine, and Phospho-Serine. The side chain of the amino acid present at the S155 position appears to be of importance in DDR signalling. This figure compares the structure of the side chain of the studied amino acids. A) Serine is present at the 155 site in WT Ku70. Serine has an OH functional group as its side chain. B) The OH of a serine is a common site for phosphorylation. C) Alanine has no side chain, meaning that when it is incorporated at a site in place of serine there is no longer the opportunity for phosphorylation. D) Aspartic Acid has a side chain that resembles a phosphorylated serine group in structure and size and is therefore considered a phosphomimetic.

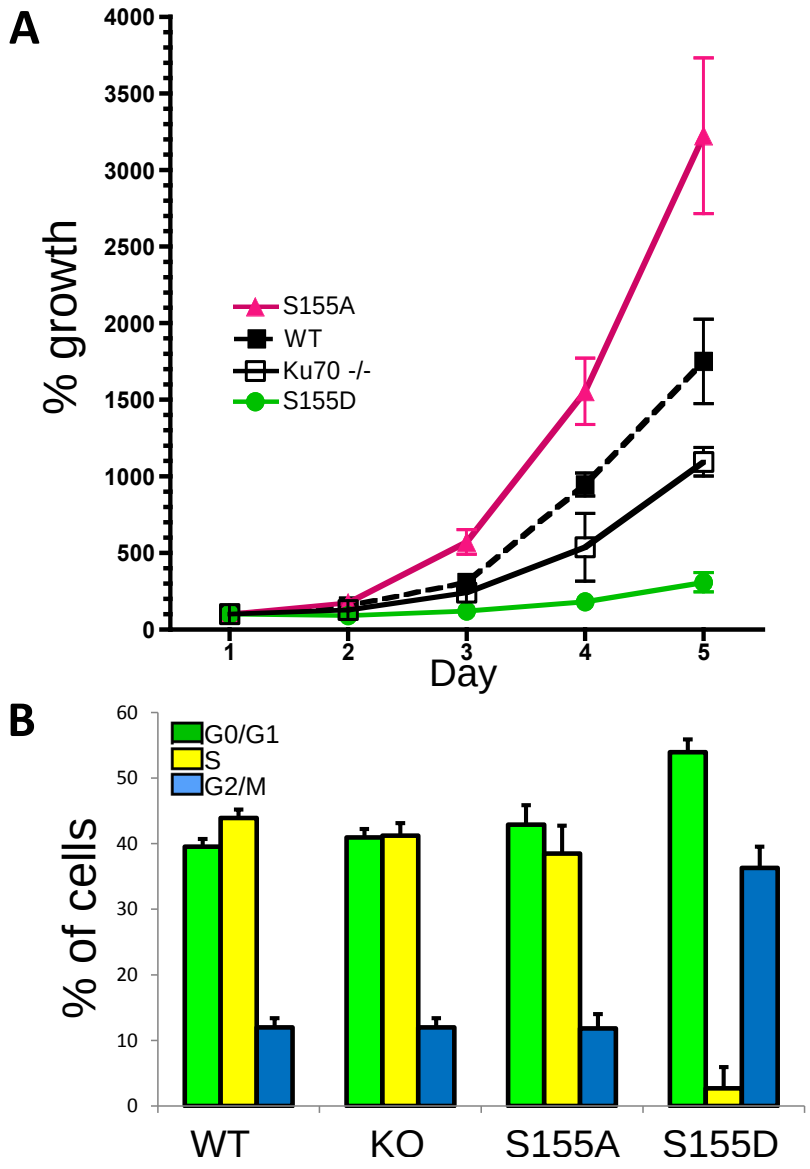

Figure 1.5: Ku70 mutants exhibit altered proliferation and cell cycle profiles. A) S155 mutants display abnormal growth rates in normal culturing in absence of DNA damage. S155 mutant expressing MEFs were plated at equal density then cells were counted on each day for 5 days, with growth rate shown as a percentage of day 1. S155A expressing MEFs proliferate at a significantly faster rate than WT MEFs. Ku70 S155D MEFs do not proliferate. B) Ku70 S155D expressing MEFs arrest in G1 and G2 phases. Flow cytometry analysis of Ku70 MEFs measuring propidium iodide content and EdU incorporation in order to determine the percent of cells in each stage of the cell cycle based on DNA content. This figure was adapted from: Ku70 Serine 155 mediates Aurora B inhibition and activation of the DNA damage response in Scientific Reports by Fell *et. al.* [91].

1.7 Aurora B kinase

In a pull-down screen for proteins interacting with Ku70 S155D, Aurora B kinase was identified [91]. This interaction was verified by co-immunoprecipitatation of Aurora B with a Ku70 S155D peptide but not with a corresponding WT Ku70 peptide. In addition, Aurora B from Ku70 S155D expressing MEFs co-immunoprecipitated with Ku70, while this was not the case in WT Ku70 expressing extracts [91].

Aurora B is a well characterized serine/threonine mitotic kinase as well as being a member of the Aurora Kinase family [92]. This small group of kinases consists of 3 human proteins: Aurora A, Aurora B, and Aurora C [93]. Aurora A and B are similar in structure but have distinct functions within mitosis throughout the body, while Aurora C, which is structurally even more similar to Aurora B, is found almost expressed primarily in the testes [92]. These proteins each have distinct roles. Deregulation of these kinases leads to polyploidy and has been linked to tumour progression [93, 94]. Therefore, these Aurora kinases are putative antitumour treatments, specifically because they regulate cell division, a key step in the development and progression of tumours [93]. Encouraging results have been shown with the Aurora kinase inhibitors [95, 96, 97].

Aurora B specifically, was originally identified in *Drosophila* where a mutated form led to monopolar spindles which in turn led to its naming after the Aurora Borelalis [94]. Aurora B acts in mitosis as the catalytic subunit of the chromosomal passenger complex (CPC) [94, 98]. In addition to Aurora B, there are 3 other core members of the CPC: INCENP which provides a scaffold basis for the complex and aids in Aurora B activation, Survivin which aids in targeting of the complex and has a debated role in inhibiting apoptosis, and Borealin which aids in directing localization of the complex [92, 93, 98]. There is an additional fifth chromosomal passenger, telophase disc-60 kD (TD-60), which is necessary for the full activation of Aurora B kinase activity [99]. This complex has been demonstrated to move throughout the nucleus playing a role in many of the crucial stages of mitosis progression. Specifically, Aurora B, in the CPC, plays a role in: phosphorylation of Histone H3 and related chromosome condensation, chromosome-microtubule interactions, spindle assembly, centromeric cohesion, and cytokinesis [92, 93, 98].

Although levels of Aurora B appear to be low in G1, Aurora B has been demonstrated to be expressed and have functions outside of mitosis [100, 101]. Aurora B has been identified as a regulator of the G1/S cell cycle checkpoint in a mTOR signalling dependent manner [100].

Additionally, it has been shown to regulate the postmitotic checkpoint and endoreplication through phosphorylation of Retinoblastoma protein (Rb), which can lead to polyploidy when cells are treated with an Aurora B inhibitor [101]. Aurora B also acts at the G2/M checkpoint where it phosphorylates the transcription factor Yin Yang 1 (YY1) [102]. Also at the G2/M checkpoint, Aurora B acts in the phosphorylation of Histone H3 and it appears that this activity regulates the dissociation of Heterochromatin Protein 1 (HPA1α) from heterochromatin [103]. Interestingly, Ku70 has been demonstrated to interact with HP1α in a yeast two-hybrid screen [104]. These functions of Aurora B suggest that it may play functions outside of mitosis and specifically at cell cycle checkpoints.

In addition, Aurora B and the DNA damage response have been previously linked through Aurora B phosphorylation of ATM, a key kinase of the DDR [105]. This phosphorylation on Ser1403 of ATM, by Aurora B, leads to its activation in mitosis independent of the DNA damage state of the cell [105]. In a thiophosphate labelling screen for targets of Aurora B, many chromatin associated proteins were identified as expected, but in addition somewhat unexpectedly, some DNA damage response proteins were identified [106]. Specifically Telomere-associated protein RIF1, FACT complex subunit SPT16, and DNA-PKcs [106]. Additionally, Aurora B has been demonstrated to play a role outside of mitosis in the phosphorylation of p53 leading to ubiquitin-dependent p53 degredation [107, 108]. This activity of Aurora B decreases p53 transcriptional activity [107] and therefore also decreases p53-activated cell cycle arrest as outlined in the DDR section and Figure 1.2. In summary, it appears that in addition to roles in directing mitosis, Aurora B may also play a role in the DDR.

The identification of Aurora B as interacting with a Ku70 S155D peptide and Ku70 S155D by co-immunoprecipitation but not with the corresponding WT Ku70 was intruiging because of the previously stated function of Aurora B in the regulation of the cell cycle and its association with key proteins in the DDR. In addition, further testing and literature review demonstrated that chemical inhibition of Aurora B shows many of the same phenotypes as expression of the Ku70 S155D mutant. For example, treatment with inhibitors of the Aurora kinases, specifically VX-680, causes endoreplication, induction of p21 expression, arrest in the G1 (or pseudo G1) state, reduction in Histone H3 phosphorylation, and activation of DNA damage response markers such as 53BP1 and γH2AX foci [91, 95, 109, 110]. Similarly, Aurora B knockout cells showed a decreased entry into S phase (supporting cell cycle arrest at the G1 cell cycle checkpoint), premature mitotic exit, induction of p21 expression, and defective Cdk1 activity [111]. Gizatullin and colleagues additionally show that siRNA depletion of Aurora B alone caused a small increase in the proportion of cells with G2/M DNA content. Overall, the con-

stitutive activation of ATM, induction of p21, cell cycle arrest, and presence of DNA damage markers seen upon expression of Ku70 S155D were also present upon inhibition of Aurora B [91].

Additionally, micro-irradiation experiments in the work by Fell *et. al.* (2016) demonstrate that Aurora B is recruited to sites of DNA damage. This change in localization supports that Aurora B may play a role in the signalling following DNA double strand breaks, as much of the initial signalling occurs in proximity to the break.

1.7.1 Regulation of Aurora B

The activity of Aurora B is regulated by many different proteins. From interaction with co-factors in the CPC, such as INCEP, to phosphorylation by kinases such as CHK1, Aurora B requires many other proteins to become fully activated [92]. As proof of this, Hengeveld and others showed that bacterially expressed Aurora B is not sufficient to phosphorylate Histone H3 in a *in vitro* kinase assay [106]. However, endogenous Aurora B immunoprecipitated from cells does phosphorylate Histone H3 in a similar *in vitro* kinase assay [91, 106].

Additionally, there are a number of proteins that have been demonstrated to inhibit Aurora B activity. Specifically, phosphatases such as protein phosphatase 1 (PP1) and protein phosphatase 2A (PP2A) both bind to and inhibit Aurora B kinase activity [92]. Futhermore, the PP1 based inhibition of Aurora B, is dependent on ATM phosphorylation of I-2 (inhibitor-2) leading to its dissociation from PP1 [55]. In an opposing pathway, PP1 and PP2A control the threshold for DNA damage reponse activation through regulation of ATM activation [54]. Similar work by Monaco and colleagues, showed that Aurora B is inhibited in response to DNA damage. These authors demonstrate that this is due to DNA damage dependent activation of poly(ADP-ribose) polymerase (PARP)1, and subsequent pol(ADP-ribosyl)ation of Aurora B [112]. This work proposes additional links between Aurora B regulation and DNA repair and the DNA damage response pathways.

Since Aurora B is highly regulated, had been previously associated with DNA damage response and repair pathways, and its chemical inhibition led to similar phenotypes as the expression of Ku70 S155D, Fell and colleagues proposed that Ku70 phosphorylation, or expression of the phosphomimetic Ku70 S155D, could lead to the inhibition of Aurora B [91]. Both *in vitro* and *in vivo* kinase assays for Aurora B activity (phosphorylation of Histone H3) demonstrated that Aurora B in Ku70 S155D expressing cells had lower kinase activity than

Aurora B in WT Ku70 expressing cells [91]. This supports that Ku70 S155D inhibits Aurora B kinase activity leading to DDR activation.

1.8 Hypothesis and objectives

Based on this work, I hypothesize that Ku70 S155D mimics phosphorylation of Ku70 in response to damage, and that Ku70 S155D and the corresponding phosphorylation of Ku70 S155 are able to inhibit Aurora B leading to a sustained activation of the DDR and cell cycle arrest through activation of DDR signalling. The main goal of this work is to determine how phosphorylated Ku70 is able to inhibit Aurora B and mediate the DDR and cell cycle arrest, through experimentation using the phosphomimetic Ku70 S155D. A theoretical model of how Ku70 S155D phosphorylation may act in DNA Damage response is shown in Figure 1.6.

The plan for this project involves 3 objectives: The first objective is to investigate the functional properties of Ku70 S155 mutant re-expression in Ku70$^{-/-}$ cells. The second objective is to characterize the role of Ku70 S155D in inhibition of Aurora B and the activation of the DDR. The final objective is develop a Ku70-inducible expression system.

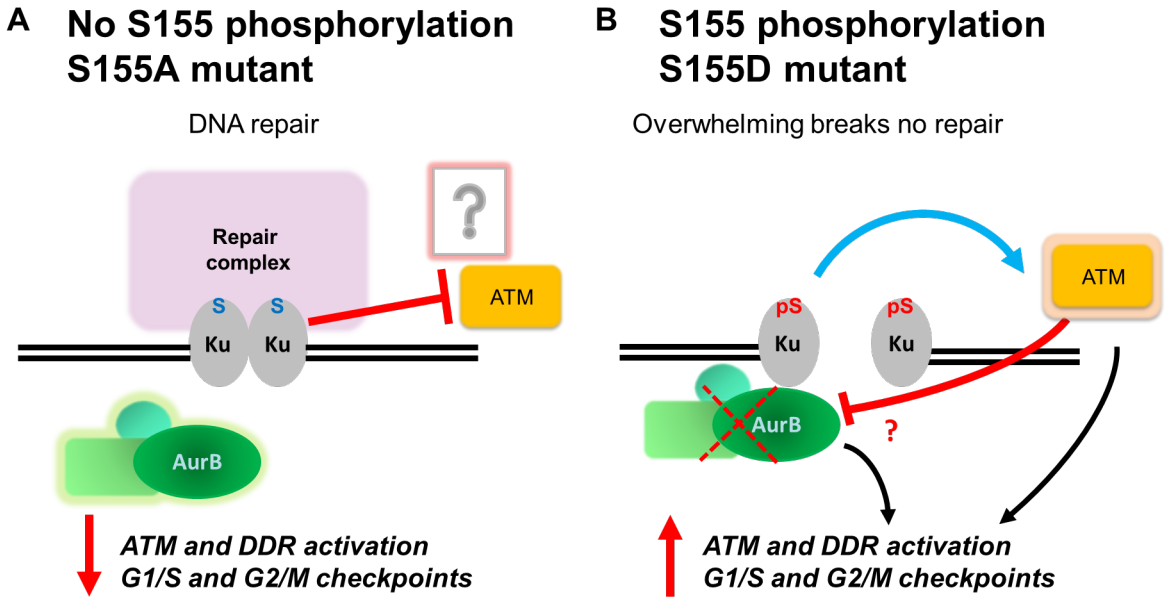

Figure 1.6: Hypothetical model for the cells response to DNA damage through Ku70 phosphorylation. Following DNA damage Ku initiates repair through recruitment of the repair complex. A) We propose that if DNA repair is completed, Ku70 S155 does not become phosphorylated and no Aurora B inhibition occurs. In this context we propose that some factor, such as ATM, is not activated and leaves Aurora B fully functional. B) In the case of persistent or overwhelming DNA damage, we propose that Ku70 is recruited to the break and becomes phosphorylated. This phosphorylation is mimicked in our studies through expression of Ku70 S155D. In the case of Ku70 S155D expression or phosphorylation of Ku70, some factor, such as ATM, is activated to inhibit Aurora B. This phosphorylation of Ku70 also then leads to the DDR and cell cycle checkpoint activation phenotype.

Chapter 2

Methods

This chapter outlines the materials used in this work and the specifics of the procedures followed to complete the experiments.

2.1 Plasmid constructs

Full length Ku70 WT, S155D and S155A were previously cloned into the pMSCVpuro vector for infection into mammalian cell lines [90].

WT Ku70-HA was created using the pMSCVpuro WT Ku70 construct as a template for polymerase chain reaction (PCR). The DNA was amplified with a forward primer at the beginning of Ku70 and a reverse primer which removed the stop codon and introduced a C-terminal HA-tag as well as an EcoRI cut site (See primer table: Table A.1 (Appendix)). Digestion of this PCR product with EcoRI cuts after the HA-tag and within Ku. This fragment was then used to swap out the C-term in WT Ku70 pMSCVpuro, thereby introducing the HA-tag. To create the mutants PSI and XhoI enzymes were used to swap the middle section of Ku70 from the previously made Ku70 pMSCVpuro mutants into the new WT Ku70-HA construct.

The Ku70 WT and S155D vWA fragment for bacterial expression was created by Dr. Victoria Fell using PCR primers to produce a fragment (aa 1-252) of Ku70 from the full length pMSCVpuro construct. This N-term fragment was subcloned into the pET-28-a (Novagen, Millipore) expression vector.

A tetracycline repressible system was created by cloning full length (FL) Ku70 WT and S155D into the pBIG2r vector [113]. Ku70 was PCR amplified from the pMSCVpuro constructs using primers with additional restriction enzymes sites (See Table A.1 (Appendix)). These FL Ku70 WT and S155D PCR fragments were then inserted into the multiple cloning site of the pBIG2r vector, creating an expression vector that could be transfected into mammalian cell lines and would allow for tetracycline repression of Ku70 expression.

2.2 Cell culture

All cell types were cultured in Dulbecco's Modified Eagle's Medium (DMEM), supplemented with 8% fetal bovine serum (FBS), 1% sodium pyruvate, and 1% glutamine (Wisent, St. Bruno, Quebec, Canada) at 37^oC and under 5% CO_2. For MEFs, media was additionally supplemented with 0.05% 2-mercaptoethanol (Sigma-Aldrich, Oakville, Ontario, Canada). HeLa cells were cultured in DMEM.

Ku70 knockout ($Ku70^{-/-}$, KO) MEFs were obtained from S. Matsuyama (Case Western, Cleveland [114]) and were retrovirally infected with pMSCV containing WT or mutant Ku70 (S155A or S155D) or empty pMSCV vector. This was done as previously described [90] using the primed media from Phoenix-AMPHO Human Kidney cells (ATCC CRL-3213) transfected with the constructs to create the viral packaging for MEF infection. Once infected, MEFs were maintained under 2.5 μg/mL puromycin.

Phoenix-AMPHO cells were also transiently transfected with Ku70-HA constructs to show interactions with Ku80 (see Transfections).

$Ku70^{-/-}$ MEFs were transfected with Ku70 WT and S155D constructs in the pBIG2r expression vector (see Transfections). Stable integration was selected for by treatment with 300 μg/mL of Hygromycin-B (Wisent) at 24 h after transfection and the suppression of the expression of Ku70 was achieved by the addition of 6 μg/mL of tetracycline (Bioshop) at 4 hours after transfection. In order to induce Ku70 expression, the media above the cells was removed, cells were washed in phosphate buffered saline (PBS)(Wisent) and DMEM with hygromycin but without tetracycline was added.

2.2.1 Cell culture treatments

For all treatments, cells were seeded at least 1 day prior to treatment. Plates of cells were treated at a confluency in the range of 70-90%.

Transfections

Transfection of Pheonix-Ampho cells was done using Calcium phosphate reagents: 0.13M $CalCl_2$ in HBS (25 mM Hydroxymethyl piperazineethanesulfonic acid (HEPES) pH 7.4, 140 mM NaCl, 6 mM Dextrose, 0.75 mM Na_2HPO_4, and 5 mM KCl)[90]. These cells were then harvested after 24 hours or the media above the cells was used to infect MEFs (as previously described [90]).

Transfection of MEFs with the pBIG2r Ku70 constructs was done using with JetPrime transfection reagent and buffer (PolyPlus Transfection, Illkrich, France). 8 μg of DNA was used to transfect a 10 cm plate of Ku70 KO MEFs. Plates were then subjected to selection using hygromycin and Ku70 expression was suppressed with tetracycline (See tissue culture section above).

Irradiation

DNA damage was induced by X-ray irradiation of cells using a Faxitron RX-650 X-ray cabinet (Faxitron X-ray LLC, Lincolnshire, IL, USA). Depending on the experiment, cells were irradiated at 1-40 Gy using a dose rate of 1.42 or 3.75 Gy/min.

Aurora B chemical inhibition

The Aurora B specific inhibitor AZD-1152 (Sigma-Aldrich) was diluted in Dimethyl sulfoxide (DMSO) and used at a final concentration of 20 nM in culture (20 μM stock diluted 1:1000 in media). Inhibitor or DMSO vehicle was added to Ku70 WT and S155D expressing MEFs, which were then incubated for 24 hours before fixation for immunofluorescent assay.

2.3 Nuclear extracts

To exclusively collect nuclear proteins, cells were washed with PBS and scraped into PBS for collection of cell pellets by centrifugation. Cell pellets were resuspended in NE Buffer A (10 mM HEPES pH 7.9, 1.5 mM $MgCl_2$. 10 mM KCl) supplemented with 0.5 mM DTT and 0.2 mM PMSF and incubated for 10 minutes on ice. NP-40 was added to the solution to a final concentration of 0.2%. The solution was then centrifuged to collect the pellet containing nuclei. The supernatant containing the cytoplasmic fraction was removed and the pellet was resuspended in NE Buffer C (20 mM HEPES pH 7.9, 25% glycerol. 450 mM NaCl, 1.5 mM $MgCl_2$, 0.2 mM EDTA) supplemented with fresh inhibitors (0.2 mM phenylmethane sulfonyl fluoride (PMSF), 1 mM Dithiothreitol (DTT), 1 g/mL leupeptin, 10 g/mL aprotinin, 1 g/mL pepstatin, 1 mM Sodium fluoride (NaF), and 1 mM Sodium orthovanadate (Na_3VO_4))(Obtained from BioShop, Burlington, Ontario, Canada). Finally, nuclear extracts were collected from the supernatant following a 5 minute centrifugation at 13,000 rpm at 4^oC. Extracts were quantified using Bradford assay and were stored at -80^oC.

2.4 Antibodies

Antibodies were used for western blot analysis, immunofluorescence assay, and immunoprecipitation. A list of relevant antibodies, their dilutions for use, and where they were obtained from is available in Table B.1 (Appendix).

2.5 Immunoprecipitation

To prepare extracts for immunoprecipitation (IP), nuclear extracts were diluted 1:3 in No Salt Co-IP Binding Buffer (25 mM HEPES pH 7.9, 0.5 mM EDTA, and 12% glycerol) supplemented with inhibitors (PMSF, DTT, leupeptin, pepstatin, aprotinin, NaF, Na_3VO_4), at the same concentrations as for nuclear extracts. Extracts were pre-cleared with 3 μL of pre-washed Protein G magnetic beads (EMD Millipore, Billerica, Massachusetts, USA) with agitation at 4^oC for 30 minutes. The beads were removed and the antibody for immunoprecipitation was added to the extract (0.1 μg of antibody for every 100 μg of protein extract) and incubated for 2 hours at 4^oC with agitation. To capture the antibody and it's bound proteins, 10 μL of pre-washed

Protein G magnetic beads were added to the solution for a 1 h incubation. Beads were then precipitated using a magnetic rack, and were subsequently washed using Co-IP binding buffer (No Salt Co-IP binding buffer supplemented with 0.1% NP-40 and 60 mM KCl). Immunoprecipitates were then ready for use in kinase assay or to be analyzed by western blot.

2.6 Western blotting

Western blots were performed by subjecting proteins to sodium dodecyl sulfate polyacrylamide gel electrophoresis (SDS-PAGE) on gels ranging from 8-15%. Samples were prepared by adding 1/6 the total volume of SDS loading dye (0.35 M Tris pH 6.8, 12% SDS, 30% Glycerol, 600 mM DTT, 0.06% bromophenol blue)and boiling. Following protein separation, the gel was equilibrated in semi-dry transfer buffer (50 mM Tris, 40 mM glycine, 20% methanol) for 10 minutes. In parallel, a polyvinylidine difluoride (PVDF) membrane was prepared by dipping in methanol then equilibrating in semi-dry transfer buffer. Western blotting was carried out in a Bio-Rad Trans-Blot Turbo transfer system (Bio-Rad, Mississauga, Ontario, Canada), with three pre-soaked filter papers on each side of the gel-membrane transfer. Transfers were done at 2.5 amperes and 25 volts for 25 minutes.

Following transfer, the membrane was blocked in 5% non-fat dry milk powder (No Name brand) prepared in Tris Buffered Saline (50 mM Tris-Cl, pH 8; 150 mM NaCl) + 0.05% Tween-20 (TBS-T). The membrane was subsequently incubated, for 1 h at room temperature or overnight at 4^{o}C, with primary antibodies diluted in 5% milk in TBS-T (See Table of antibodies for identities and dilutions). The blot was washed three times using Tris buffered saline-Tween-20 (TBS-T), and was incubated with species specific secondary antibodies, washed three times, and developed using Clarity Western ECL substrate (Bio-Rad, Mississauga, Ontario, Canada). Image exposures of western blots were collected using a Molecular Imager ChemiDoc XRS system and the associated Image Lab Software (Bio-Rad, Mississauga, Ontario, Canada).

In addition to creating images for publication, the Image Lab software was also used for the quantification of protein bands on western blots.

2.7 Immunofluorescence assay

Immunofluorescence assay was performed by first seeding MEFs on coverslips. One day after seeding, or following treatment, cells were washed three times in PBS and were fixed onto coverslips using 3% paraformaldehyde (BioShop). The coverslips were then washed again three times and stored a 4^oC. Next, 0.5% Triton X-100 (BioShop) was used to permeabilize the cells, and was washed off with 3 subsequent washes of PBS. Cells were then blocked in 5% FBS (Wisent) prepared in PBS. Coverslips were incubated overnight at 4^oC with light agitation in primary antibody prepared in 5% FBS (See Table of antibodies for identities and dilutions). Primary antibody was washed off in PBS washes and coverslips were then incubated with species-specific, AlexaFluor 488/647 secondary antibodies (Invitrogen). Secondary antibodies were used at a 1:1000 final dilution in 5% FBS solution. Antibody was washed off in PBS washes, and coverslips were briefly air dried before mounting on glass slides with Prolong Diamond Antifade Mountant with 4',6-diamidino-2-phenylindole (DAPI) (ThermoFisher Scientific, Rockford, Illinois USA).

Imaging for immunofluorescence assay was completed at 20 or 40x magnification with an Olympus BX51 microscope (Olympus Corporation, Tokyo, Japan) and with Image-Pro Plus software (Media Cybernetics, Rockville, Maryland, USA). Images were analyzed and prepared with ImageJ software [115].

2.8 Comet assay

Comet assays were conducted to assess DNA damage. Ku70 S155D or WT expressing MEFs were either untreated, irradiated over a range of doses, or treated with hydrogen peroxide (H_2O_2) in preparation for comet assay. They were subsequently stored on ice before harvesting by scraping in PBS. Cells were counted using a hemocytometer and diluted in PBS to a final concentration of 1 x 10^5 cells/mL. From this solution, approximately 3000 cells were diluted 1:10 in low melting point agarose and mounted on slides.

2.8.1 Neutral comet assay

Neutral comet assay was done using the Enzo Comet SCGE assay (Cedarlane, Burlington, Ontario, Canada). The protocol described by the manufacturer was followed. Briefly, Ku70 WT and S155D expressing cells were compared to WT expressing cells that were treated with 100 μM of H_2O_2 or 40 Gy of irradiation and incubated on ice immediately to prevent DNA repair. Cells diluted in PBS were mixed with 1% low melting point agarose which was cooled to set on coated coverslips, creating a gel matrix with cells embedded in it. These cells were then subjected to lysis buffer and electrophoresis. Slides were dried and incubated with CYGEEN which stains nucleic acids. This staining allowed for visualization using the Olympus BX51 microscope.

2.8.2 Alkaline comet assay

For the alkaline comet assay, Ku70 WT and S155D expressing MEFs were compared to WT expressing MEFs treated with a range of irradiation doses (1-10 Gy). The cells suspended in PBS were mixed with 1% agarose and mounted on slides that were precoated with 0.6% agarose. The rest of the procedure was carried out in the dark. The cells suspended in agarose were lysed in Lysis Buffer (2.5 M NaCl, 0.1 M EDTA, 10 mM Tris, 1% DMSO, 1% Triton X-100, pH 10 (NaOH)) for 1 h at 4^oC. Slides were then washed 3 times in cold water, incubated for 45 minutes in alkaline electrophoresis buffer (1 mM EDTA, 50 mM NaOH, 1% DMSO), and subsequently electrophoresed for 10 minutes at 18 V. Next, the slides were neutralized in 0.4 M Tris buffer (pH 7.0) for 30 minutes at 4^oC. Finally the DNA from the cells was stained with CYGREEN solution allowing for comets to be visualized and analyzed using the Olympus BX51 microscope.

2.8.3 Comet assay analysis

Once images were taken, the mean tail moment of comets were measured using the OpenComet plugin for ImageJ software. The mean tail moment was taken for at least 200 cells per experimental treatment, was averaged, and was normalized to the mean tail moment of the untreated WT cells for that experiment.

2.9 Proximity ligation assay

Proximity ligation assay (PLA) was done for the co-localization of Ku70 and Aurora B in MEFs stably infected with Ku70 WT, Ku70 S155D, or empty vector (KO). Cells were seeded the night before on coverslips that had a hydrophobic circle around the outer edge. Cells were fixed, permeabilized, and blocked as described in the Immunofluorescence Assay section. They were then incubated overnight at 4^{o}C with primary antibodies mouse anti-Ku70 (N3H10, Santa Cruz) and rabbit anti-Aurora B (H-75, Santa Cruz). After removal of primary antibodies and washing in PBS, the cells were incubated with PLA probes: anti-mouse minus and anti-rabbit plus (Sigma-Aldrich). The ligation and amplification steps were then completed as described by the manufacturer (Duolink Kit, Sigma-Aldrich). Coverslips were briefly dried and mounted using DAPI-mounting medium. Images were acquired and prepared as described in the Immunofluorescence Assay section. The PLA signal was quantified using ImageJ to calculate image intensity and this was divided by the number of cells in each image. This value was then normalized to the PLA signal of the Ku70 KO cells.

2.10 Bacterial protein expression

Ku70 WT and S155D vWA domains were expressed in *Escherichia coli* (*E. coli*) cells for later testing for inhibition of Aurora B. The vWA domains in pET-28-a were transformed into chemically competent BL23(DE3) *E. coli* cells. Bacteria were cultured at 37^{o}C. Transformants were used to innoculate a 2 mL Lysogeny broth (LB) overnight culture, which in turn was used to spike a 200 mL LB day culture. After 2-3 hours, when the culture reached an optical density (600 nm) of approximately 0.5, protein expression was induced with 1 mM of Isopropyl β-D-1-thiogalactopyranoside (IPTG) and cultures were grown for an additional 1.5 hours. A brief centrifugation was used to harvest a cell pellet, which was frozen and then lysed using sonication in Lysis Buffer (10 mM KCl, 25 mM HEPES pH 7.4, 2 mM EDTA, 20% glycerol, and 0.1% NP-40 with inhibitors added as in Whole Cell Extracts). Finally, the cell debris and soluble protein fractions were separated by centrifugation, and protein expression of each vWA domain was checked and quantified by SDS-PAGE analysis before being added to kinase assay reactions.

2.11 Aurora B kinase assay

Immunoprecipitated Aurora B on magnetic beads was diluted in Kinase buffer (20 mM Tris-HCl, 20 mM KCl, 20 mM $MgCl_2$, 100 mM ATP (New England Biolabs, Ipswich Massachusetts, USA), 0.4 mM DTT) and divided into 7 aliquots. One aliquot remained as a control, to the other 6 aliquots increasing amounts of bacterially-expressed T7-tagged Ku70 S155D or Ku70 WT vWA domain (1, 5, and 10 ng) were added. These were incubated for 30 minutes at 4^oC, following which 1 μg of Histone H3 (New England Biolabs) was added and the solution was incubated for an additional 30 minutes at 37^oC. Finally, SDS loading dye was added to samples and they were analyzed by western blot (see above) with antibodies against Aurora B, T7-tag, and phosphorylated Histone H3.

2.12 Statistical analysis

Bar-graph results are represented with standard error of the mean (SEM) error bars. Calculations of error bars and T-tests for significance were performed using GraphPad (GraphPad Software, Inc., La Jolla, California, USA). Results were considered significant if analysis by t-test resulted in a p-value less than 0.05.

Chapter 3

Results

3.1 Ku70 S155D expressing cells have low level DNA damage similar to that of WT

The research leading up to this work showed the presence of a DNA damage response upon the expression of Ku70 S155D [91]. It was suggested that this response occurred as the result of the mutant mimicking Ku phosphorylation and activating a DDR signalling pathway. However, although improbable because of Ku's well characterized DNA repair function, it was also possible that this DDR was activated as a response to actual DNA breaks induced by the Ku70 S155D expression. To test whether Ku70 S155D expression induces DNA damage, I expressed Ku70 S155D and Ku70 WT in Ku70$^{-/-}$ MEFs using a retroviral infection system, as previously described [90], and tested for DNA damage with comet assays (Ku70 WT and S155D re-expression is demonstrated in Appendix C.1). Quantification of DNA damage was done using both alkaline and neutral comet assays which assess different types of DNA breaks and display different levels of sensitivity for DNA breaks.

Briefly, cells that were suspended in low melting point agarose were lysed then treated with neutral or alkaline conditions and an electric current was applied. In this assay, the applied electric current causes DNA to move out of the lysed cell and through the agarose gel at a speed inversely correlated with it's size. Small and medium sized DNA fragments are present if DNA damage occurred, otherwise the DNA remains as intact chromosomes. Therefore, in the presence of DNA damage, small and medium sized DNA fragments migrate out of the cell and into the agarose gel, whereas intact chromosomal DNA will remain within the cell nucleus.

When the DNA is subsequently stained, a comet-like tail is visible protruding from each cell nucleus. This effect is seen in the IR (and H_2O_2) controls for each comet assay type (Figure 3.1).

Both neutral and alkaline comet assays were performed because each has it's own strengths. The alkaline comet assay is performed under denaturing conditions, is highly sensitive, and is used to quantify the total DNA damage (single and double strand breaks and alkali-labile sites)[116]. The neutral comet assay is more specific to DNA double strand breaks, as the neutral conditions are not conducive of separating the two DNA strands, but this also means that it is less sensitive at low levels of DNA breaks [116].

The level of endogenous DNA damage in the Ku70 S155D expressing MEFs, quantified using tail moment, was comparable to that of WT Ku70 expressing MEFs in both comet assay types (Figure 3.1). Both Ku70 WT and S155D expressing MEFs had little to no DNA tail suggesting that there was little to no DNA damage. There was no significant difference in the mean comet tail moment and therefore in the measured DNA damage between the Ku70 WT and S155D cells. The endogenous DNA damage levels of Ku70 WT and S155D expressing MEFs were also compared to cells treated with exogenous DNA damaging agents including irradiation and hydrogen peroxide treatment as positive controls for the experiment (Figure 3.1). In the alkaline comet assay, increasing amounts of DNA damage were induced through irradiation over a range of 1-10 Gy, while for the neutral assay, 40 Gy and H_2O_2 were the positive control treatments. Irradiation has previously been shown to be linearly correlated with induction of DNA DSBs [18, 117]. Previous work has demonstrated that approximately 20-40 DNA DSBs are induced per cell for each 1 Gy of iraditaion dose [18, 118, 117, 119]. These controls demonstrate that upon treatment with a DNA damaging agent the comet assay is able to detect breakage, and that this breakage is relative to the treatment dose (Figure 3.1).

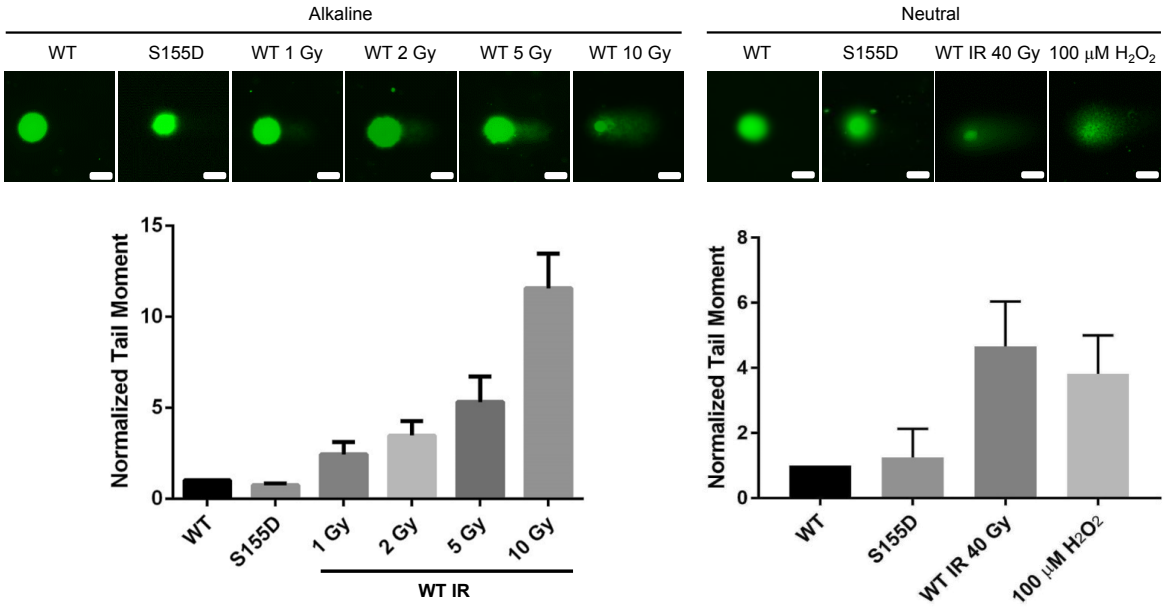

Figure 3.1: Alkaline and Neutral comet assays comparing endogenous DNA damage in Ku70 WT and S155D expressing MEFs. Untreated Ku70 WT and Ku70 S155D expressing MEFs, Ku70 WT expressing MEFs irradiated with 1 to 10 or 40 Gy respectively, and Ku70 WT MEFs treated with 100 μM hydrogen peroxide for 30 minutes were diluted and suspended in agarose gel on slides. Following lysis under alkaline or neutral conditions the slides were subjected to electrophoresis and stained with CYGREEN. Representative images (top) show DNA damage and corresponding migration. Scale bars, 10 μm. Mean tail moment was quantified for at least 100 comets using OpenComet, and mean tail moment was normalized to Ku70 WT expressing MEFs for each replicate. Normalized tail moment is shown with error bars indicating SEM (n=3).

3.2 Ku70 mutants heterodimerize with Ku80

In addition to testing for induction of DNA breaks upon expression of the Ku70 S155D mutant, we tested for the ability of the Ku70 S155D and S155A mutants to heterodimerize with Ku80. Heterodimerization of Ku70 and 80 is important in creating a dimer capable of binding to DNA DSBs. While this heterodimerization may not be necessary for the activation of the DDR, heterodimerization would support that the mutant Ku70s could still function in repair.

The S155 residue is located within the vWA domain of Ku70, which is not expected to be involved in the interaction with Ku80. However, in order to prove that the Ku70 mutants were still able to form heterodimers, Ku80 was immunoprecipitated from Phoenix-AMPHO cells that were either untransfected or transiently transfected with HA-tagged full-length (FL) Ku70 WT, S155A, or S155D. Immunoprecipitates were analyzed by western blot using antibodies against Ku80 and HA-tag. The use of the HA-tagged Ku70 was necessary to detect co-immunoprecipitation of transfected Ku70 and not the endogenous WT Ku70 found in Phoenix-AMPHO cells.

The results show that HA-FL Ku70 WT, HA-FL Ku70 S155A, and HA-FL Ku70 S155D all co-immunoprecipitate with Ku80 (Figure 3.2). This confirms that mutation of the S155 residue does not disrupt heterodimerization of Ku70 with Ku80, and specifically demonstrates that the over-expressed, transfected HA-Ku70s are capable of replacing endogenous Ku70 in the heterodimer.

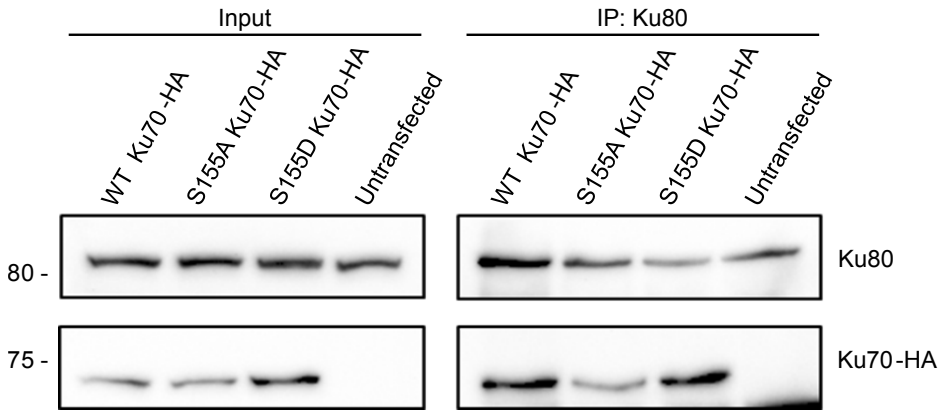

Figure 3.2: Co-immunoprecipitation of Ku70 WT and mutants with Ku80. Ku80 was immunoprecipitated from Phoenix-AMPHO cells that were untransfected or transfected with Ku70 WT, S155A, or S155D, each with an HA-tag. The western blot was prepared using primary antibodies against Ku80 and HA-tag. WT Ku70 and both mutant Ku70s co-immunoprecipitated with Ku80. (n=3).

3.3 Aurora B co-immunoprecipitates with Ku70 following IR treatment

Previous work identified Aurora B as a factor interacting with the Ku70 S155D mutant [91]. Since Ku70 S155D is hypothesized to mimic Ku70 phosphorylation in response to DNA damage, we set out to test for an association between WT Ku70 and Aurora B following DNA damage induced by X-ray irradiation. Ku70 was immunoprecipitated from $Ku70^{-/-}$ MEFs infected with WT Ku70 or empty pMSCV vector that were untreated or irradiated with 40 Gy. Immunoprecipitates were analysed by western blot with antibodies against Ku70 and Aurora B.

Aurora B co-immunoprecipitated with Ku70 from irradiated WT Ku70 expressing MEFs but not from unirradiated MEFs (Figure 3.3). This data supports that the previously characterized phosphorylation event at S155 on Ku70, which occurs in response to irradiation and is mimicked by Ku70 S155D, mediates the association of Ku70 with Aurora B.

Similarly, Ku70 was immunoprecipitated from nuclear extracts collected from HeLa cells that were either untreated, or irradiated with 40 Gy. Mouse IgG was used as a control on Hela extracts. Once again, Aurora B co-immunoprecipitated only with Ku70 from irradiated Hela extracts demonstrating that this association occurs in both mouse and human cells (Figure 3.3).

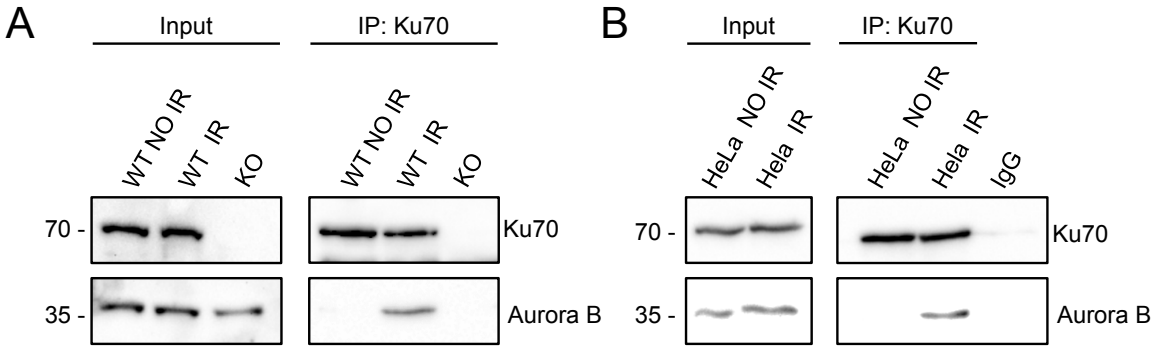

Figure 3.3: Aurora B co-immunoprecipitates with Ku70 after DNA damage. (A) $Ku70^{-/-}$ MEFs stably expressing Ku70 WT (WT) or infected with empty vector (KO) were untreated or subjected to 40 Gy of IR treatment and extracts were prepared after 30 min incubation. Immunoprecipitation was performed with a Ku70 antibody and immunoprecipitates were analyzed by western blot with antibodies against Ku70 and Aurora B. (n=3). (B) The same protocol was used on HeLa cells, with an additional control using mouse IgG. (n=2).

3.4 Ku70 S155D and Aurora B co-localize by PLA *in situ*

In addition to demonstrating the *in vitro* association of endogenous Ku70 and Aurora B following DNA damage induction using co-immunoprecipitation, we wanted to demonstrate the *in situ* co-localization of the phosphomimetic Ku70 (S155D) with Aurora B. This experiment was conducted using proximity ligation assay (PLA). The co-localization of Aurora B and Ku70 was assayed in $Ku70^{-/-}$ MEFs re-expressing Ku70 S155D or WT and in $Ku70^{-/-}$ MEFs containing pMSCV empty vector (KO). Specifically, this assay involved incubating fixed, permeabilized, and blocked cells on coverslips with mouse anti-Ku70 and rabbit anti-Aurora B primary antibodies. The cells were then washed and incubated with PLA probes against rabbit and mouse, plus and minus respectively, and treated with ligation and amplification mix from the Duolink kit.

In this assay, if the plus and minus PLA probes are within 40 nm of each other their DNA tails are ligated together to form a circular template which is then amplified through rolling circle amplification (Figure 3.3) [120]. The amplification mixture also contains fluorescently labelled oligonucleotides which are complimentary to the DNA tail of the PLA probe. Thus, following rolling circle amplification will the fluorescent probe will bind to the amplified DNA product. As a result of this process the co-localization of Ku70 and Aurora B is seen as small green dots within cells under a fluorescent microscope's fluorescein isothiocyanate (FITC) filter. In this experiment Ku70 KO MEFs were used as a negative control. In the absence of Ku70 the Ku70 antibody should not bind within the cell, while the Aurora B antibody will bind to endogenous Aurora B. Therefore, only one PLA probe will bind while the other is washed away and as a result there should be not be PLA activity.

The results show the presence of green dots within the Ku70 S155D expressing MEFs but not in Ku70 WT or Ku70 KO MEFs (Figure 3.5). This suggests that Ku70 and Aurora B co-localize in Ku70 S155D expressing MEFs and that this mutation mediates the interaction. To quantify these data, the overall intensity of each image containing PLA signal was measured using ImageJ and this value was then divided by the total number of cells in the image to give a quantitative PLA signal value. This was done for at least 150 cells for each replicate. The PLA signal value for Ku70 WT and S155D cells was then normalized to that of KO cells (Figure 3.5). Based on this PLA signal value, Ku70 and Aurora B were found to co-localize in cells expressing Ku70 S155D significantly more than in cells expressing WT Ku70 or in Ku70 KO MEFs (Figure 3.5).

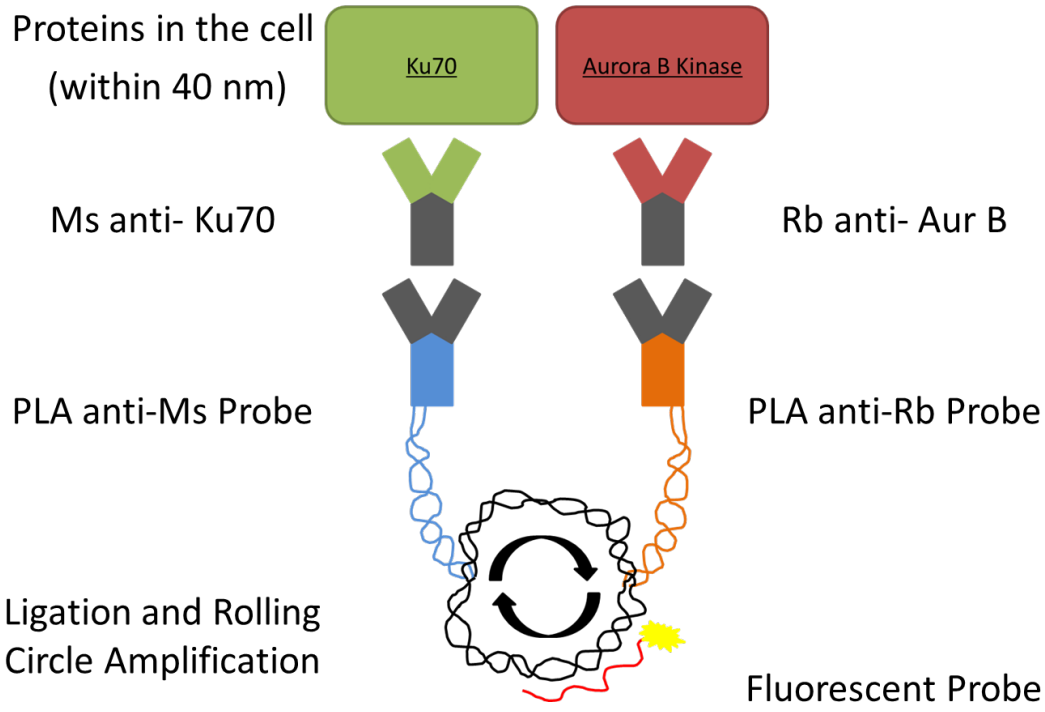

Figure 3.4: Overview of Proximity Ligation Assay (PLA). Antibodies generated in two different species against two proteins of interest are added to cells fixed on coverslips. In this experiment Ku70 and Aurora B (Aur B) primary antibodies were used. Species specific PLA probes are added and if the original proteins are within approximately 40 nm their DNA tails are ligated. Rolling circle amplification is then carried out and a fluorescently tagged oligonucleotide probe binds to the amplified DNA. The fluorescent tag can be seen using fluorescent microscopy as green green dots representing co-localization.

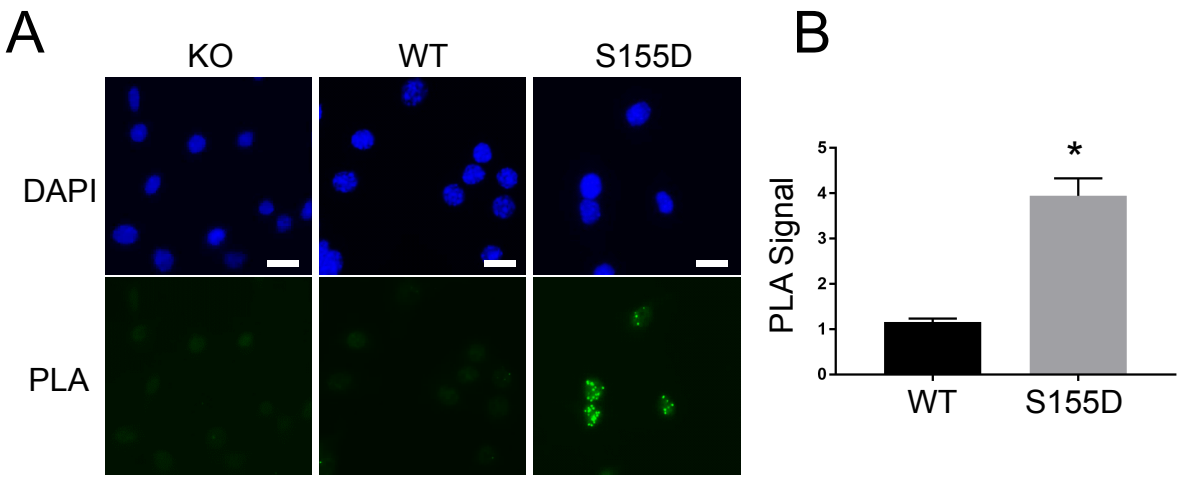

Figure 3.5: Interaction of Aurora B and Ku70 S155D using Proximity Ligation Assay (PLA). (A) Representative images for PLA co-localization of Aurora B and Ku70 *in situ*. $Ku70^{-/-}$ MEFs re-expressing Ku70 WT or S155D or infected with empty vector (KO) were fixed on coverslips and incubated with antibodies against Ku70 and Aurora B and processed for PLA analysis. With this assay, co-localization of Ku70 and Aurora B creates green dots and nuclei are stained with DAPI in blue. Images were taken with the 40x objective and scale bars represent 10 μm. (B) The PLA signal was quantified using ImageJ to calculate intensity per cell, and this was normalized to the PLA signal in the Ku70 KO cells. Quantification is shown as the average of three experiments with error bars indicating SEM. (*$p<0.05$, n=3).

3.5 Ku70 S155D vWA domain inhibits Aurora B-dependent Histone H3 phosphorylation

Since Ku70 S155D interacts with Aurora B *in situ* we sought to determine whether this plays a role in the Ku70 S155D-dependent activation of the DDR. Through the use of an *in vitro* kinase assay, previous work demonstrated that Aurora B imunoprecipitated from Ku70 S155D expressing MEFs has reduced kinase activity [91], suggesting that Ku70 S155D expression leads to Aurora B inhibition. However, this inhibition of Aurora B had not been shown to be a direct effect of Ku70 S155D expression. Since Aurora B chemical inhibition demonstrated similar effects as expression of Ku70 S155D, this inhibition merited further investigation. Interestingly, the expression of the Ku70 vWA domain alone was previously shown to efficiently activate a DDR, sugesting that that the DDR activation following Ku70 S155D expression is not dependent on DNA binding capabilities or heterodimerization with Ku80 [91].

We therefore wanted to test whether the Ku70 S155D vWA domain was sufficient to inhibit Aurora B kinase activity, which in turn could suggest a role for this inhibition in the activation of the DDR seen upon Ku70 S155D vWA domain expression. To this end, Aurora B was immunoprecipitated from Ku70 WT expressing MEFs and was divided equally into seven fractions. One fraction was left as a control, and to the others, increasing amounts of bacterially expressed T7-tagged Ku70 S155D or WT vWA domains were incubated with the immunoprecipitated Aurora B. These fractions were then subjected to an *in vitro* Aurora B kinase assay for purified Histone H3 phosphorylation.

Histone H3 phosphorylation was readily observed in the control, demonstrating robust kinase activity of immunoprecipitated Aurora B. Addition of the WT Ku70 vWA domain had a small effect in the reduction of Histone H3 phosphorylation but upon addition of the Ku70 S155D vWA domain the amount of phosphorylated Histone H3 decreased further. Quantification of the phospho-Histone H3 signal for four experiments demonstrated that while the amount of Histone H3 phosphorylation was slightly reduced non-specifically upon the addition of the WT vWA domain, there was a significantly greater reduction in the phosphorylation of Histone H3 with the addition of increased amounts of the Ku70 S155D vWA domain relative to Ku70 WT vWA addition (Figure 3.6). This reduction in phospho-Histone H3 supports the idea that the Ku70 vWA domain is sufficient to inhibit Aurora B when the S155 position is mutated to S155D.

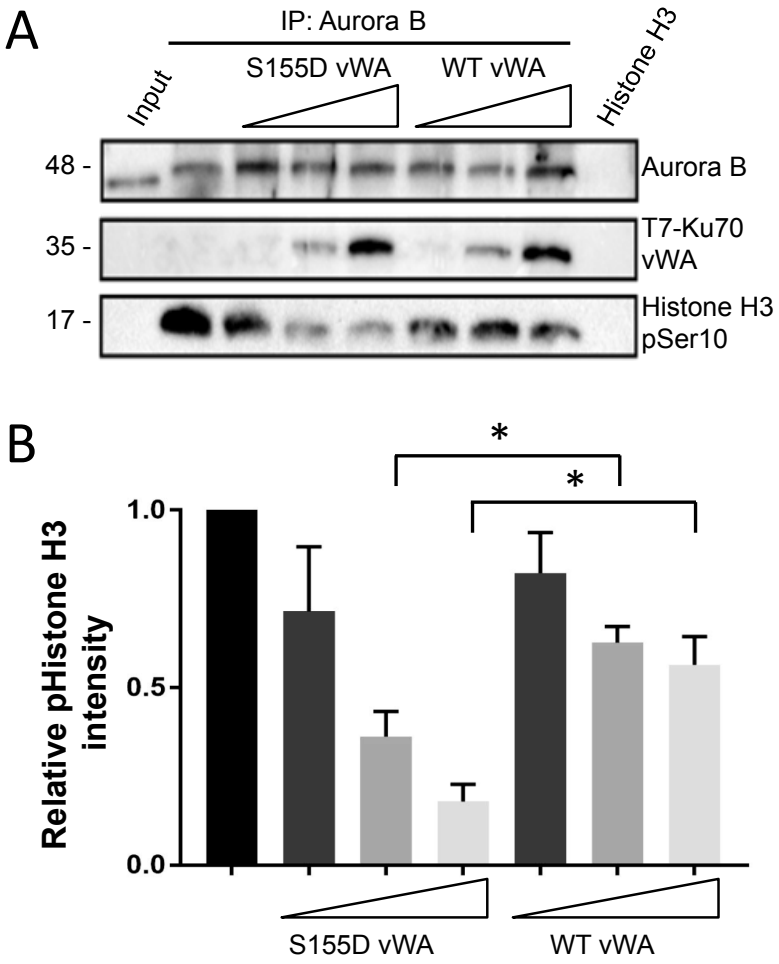

Figure 3.6: Aurora B kinase activity assay in the presence of increasing amounts of Ku70 S155D or WT vWA domain. Ku70 WT-expressing MEF nuclear extracts were immunoprecipitated with an Aurora B antibody. The immunoprecipitates were incubated with 0, 1, 5, or 10 ng of bacterially expressed, T7-tagged Ku70 S155D or WT vWA domains. A) Aurora B kinase activity was assessed using an *in vitro* kinase assay for Histone H3 phosphorylation and analyzed by western blot with antibodies to phospho-H3S10, T7 tag, and Aurora B. B) Phospho-H3S10 western blot signal was quantified relative to immunoprecipitated Aurora B and is shown as an average with error bars indicating SEM. (*$p<0.05$, n=4).

3.6 Treatment of Ku70 S155D expressing cells with an Aurora B inhibitor does not increase the activation of DNA damage response markers

Ku70 S155D expression causes the activation of the DDR and the inhibition of Aurora B, and the chemical inhibition of Aurora B results in similar effects as Ku70 S155D expression [91]. Therefore, it was postulated that the expression of Ku70 S155D could lead to the inhibition of Aurora B, which in turn causes DDR activation. However, a causal relationship between the inhibition of Aurora B and the activation of the DDR was not established. To test whether the expression of Ku70 S155D and the chemical inhibition of Aurora B phenotypes are associated, we assayed for the additive effect of treating Ku70 S155D expressing MEFs with an Aurora B inhibitor. $Ku70^{-/-}$ MEFs re-expressing Ku70 WT or S155D, were seeded on coverslips and treated with 20 nM of the Aurora B inhibitor AZD-1152 or DMSO vehicle control for 24 hours. Cell were prepared for immunofluorescence assay using an antibody against γH2AX and the nucleus was stained with DAPI. The signal was quantified as the percentage of cells with greater than 5 foci for at least 100 cells, averaged over three replicates for each treatment. For this experiment we had two possible expected outcomes: If the DDR effects of Ku70 S155D expression were due to Aurora B inhibition, then further inhibition of Aurora B would have little to no additional effects; however, if Ku70 S155D had effects on the DDR in addition to inhibiting Aurora B, then subsequent treatment with an Aurora B inhibitor would increase the DDR activation.

As expected, the percentage of cells with more than 5 γH2AX foci was significantly increased when WT Ku70 expressing cells were treated with the Aurora B inhibitor (Figure 3.7). Conversely, while the percentage of cells with more than 5 foci in untreated S155D cells was significantly increased relative to untreated WT cells, additional treatment of the S155D expressing MEFs with the Aurora B inhibitor did not further increase the response. Therefore, expression of Ku70 S155D leads to the phosphorylation of the DNA damage marker H2AX, and the phosphorylation of this DNA damage response marker is not significantly increased upon treatment with an Aurora B kinase inhibitor. This suggests that the effects are sequential and that the expression of Ku70 S155D acts to inhibit Aurora B, which in turn leads to the activation of the DDR.

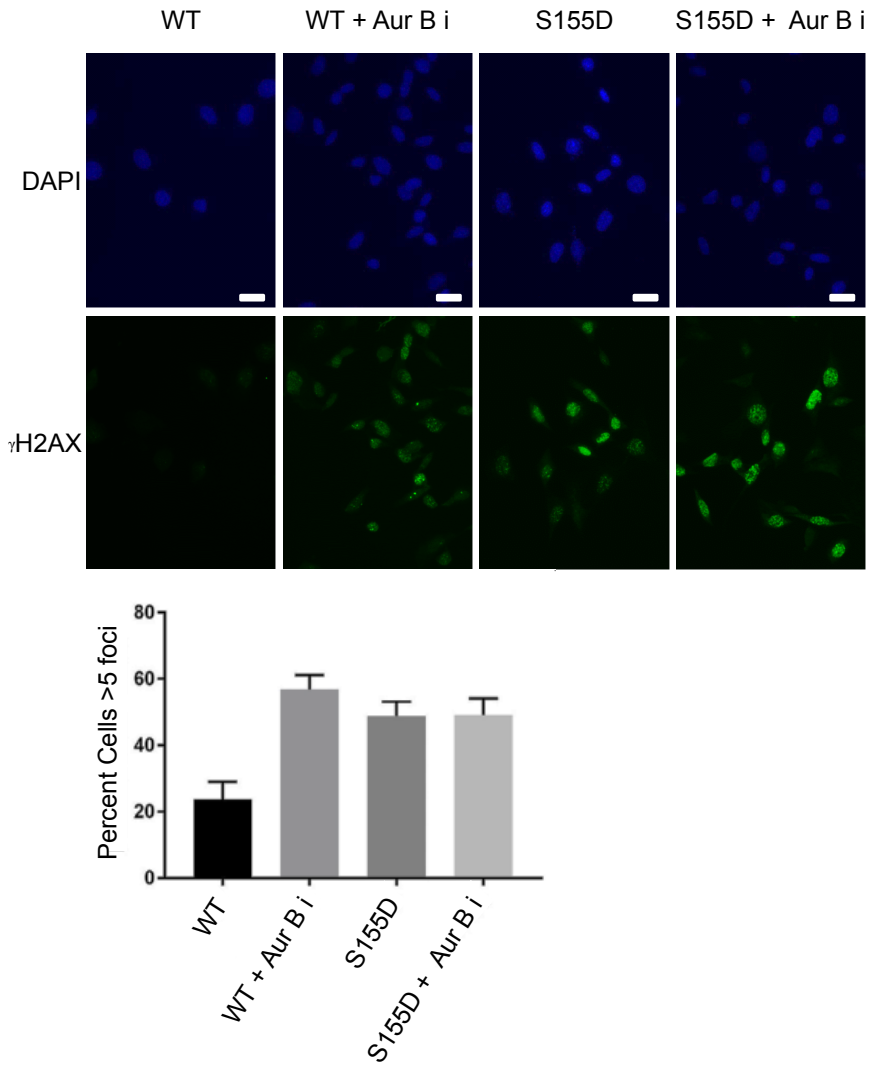

Figure 3.7: Aurora B chemical inhibition does not increase the DNA damage response in Ku70 S155D expressing MEFs. Ku70 WT and S155D expressing MEFs were seeded on coverslips and treated with 20 nM of the Aurora B inhibitor AZD-1152 (Aur B i) or DMSO vehicle control for 24 hours. Cells were then prepared for immunofluorescence analysis using an antibody against γH2AX and DAPI stain. (A) Representative photos were taken at 40x magnification and the scale bar represents 20 μm. (B) The γH2AX signal was quantified for at least 100 cells by counting the number of cell with more than 5 foci and dividing by the total number of cells to determine a percentage of cells with >5 foci per cell. There is no significant difference between the signal in Ku70 S155D expressing cells untreated or treated with the Aurora B inhibitor. Error bars represent SEM (n=3).

3.7 Establishment of a Ku70 inducible system

The expression of either Ku70 S155D or the Ku70 S155D vWA domain was demonstrated to activate the DNA damage response and cell cycle arrest [91]. However the system employed involves the selection of Ku70 S155D expressing cells for several days. This system does not allow for the detection or analysis of early events stimulated upon Ku70 S155D expression. Thus, we sought to establish an inducible system to investigate early cellular responses to Ku70 S155D expression. Tetracycline-repressible (Tet-Off) Ku70 WT and S155D constructs were created and tested. Full-length Ku70 WT and S155D were cloned into the pBIG2r vector. This vector contains a tetO element which allows for repression under tetracycline, a CMV promoter for the inserted DNA of interest, and a TK element for the tetracycline repression component [113]. Therefore, when maintained under tetracycline Ku70 should not be expressed. Addtitionally, this vector contains a selectable marker which confers resistance to hygromycin B. The pBIG2r vector containing Ku70 WT or S155D was transfected into Ku70 knockout MEFs and transfected cells were selected with hygromycin B to generate stable cell lines. These cell lines were maintained under tetracycline to repress Ku70 expression.

To demonstrate functionality and utility of this system, cells maintained under tetracycline were compared with those that had been released from tetracycline control for 2-24 hours. Before the removal of tetracycline there was consistently little to no Ku70 expression visible by western blot; while 24 h after tetracyclin removal, Ku70 was expressed from both the Ku70 WT and S155D pBIG2r constructs (Figure 3.8). Additonally, upon release from tetracycline control the amount of Ku70 in the cells gradually increased over time in both the pBIG2r WT and S155D cells (Figure 3.8). This expression was also analyzed by immunofluorescence with a Ku70 antibody. At 0 h, both S155D and WT pBIG2r containing cells had little to no Ku70 signal, while at 24h a portion of cells showed Ku70 expression (Figure 3.8). In this experiment, cells were additionally incubated with a γH2AX antibody so that the activation of the DDR in response to Ku70 WT or S155D expression could be visualized. The percentage of Ku70 expressing cells that contained more that 5 γH2AX foci was calculated for the Ku70 WT and S155D pBIG2r cells at the 8 h and 24 h post removal of tetracycline. It appears that at both time points the percentage of Ku70 expressing cells that contained more that 5 γH2AX foci was greater in the Ku70 S155D pBIG2r cells than in the WT equivalent (Figure 3.8). These results demonstrate that a Tet-Off, inducible system for Ku70 WT and S155D was established and that in this system the activation of the DDR is consistent with previous studies using infected Ku70 WT and S155D [91].

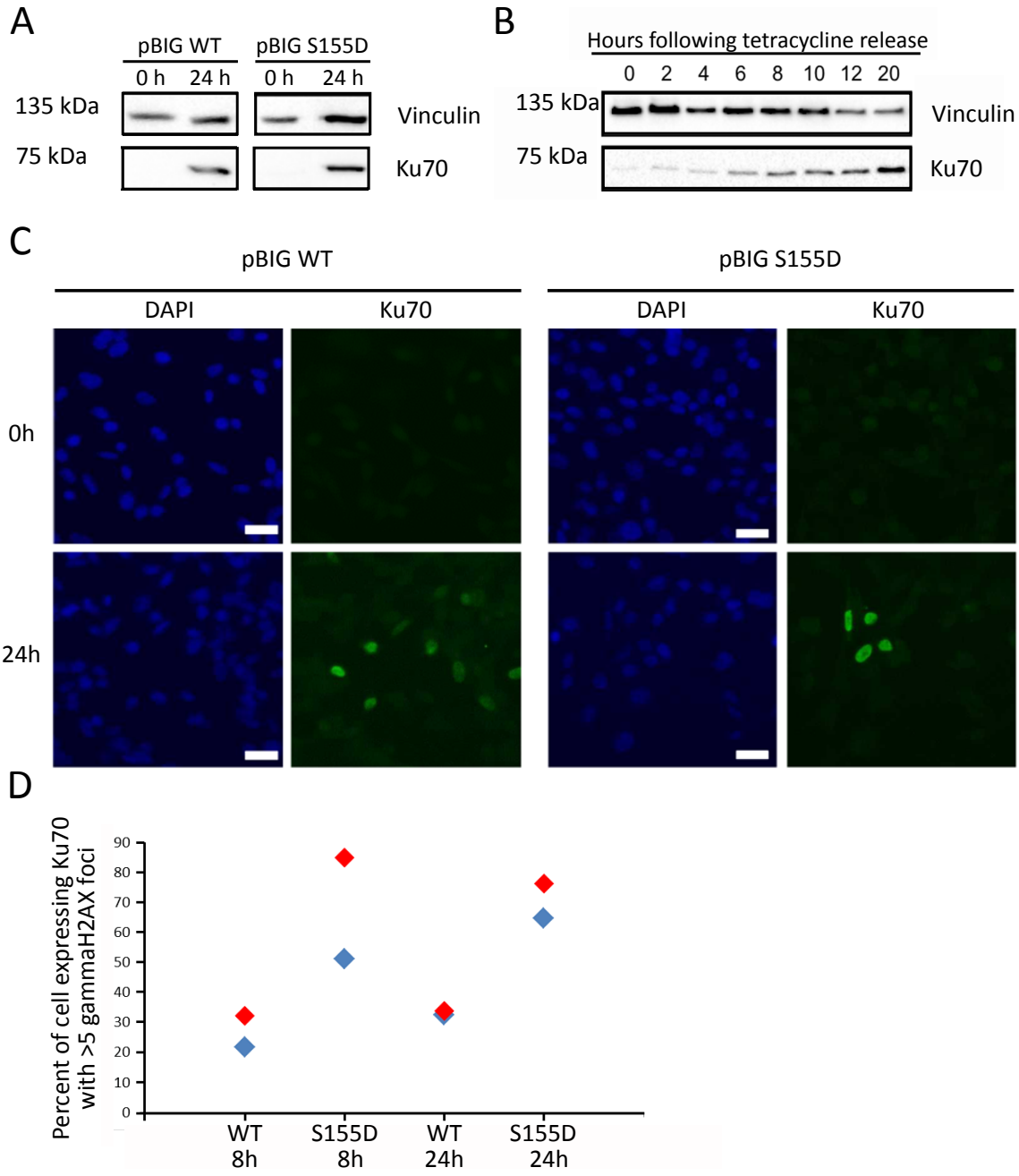
A
pBIG WT
pBIG S155D
0 h
24 h
0 h
24 h
135 kDa
75 kDa
Vinculin
Ku70
B
Hours following tetracycline release
0 2 4 6 8 10 12 20
135 kDa
75 kDa
Vinculin
Ku70
C
pBIG WT
pBIG S155D
DAPI
Ku70
DAPI
Ku70
0h
24h
D
Percent of cell expressing Ku70 with >5 gammaH2AX foci
0
10
20
30
40
50
60
70
80
90
WT 8h
S155D 8h
WT 24h
S155D 24h

Figure 3.8: Establishment of an inducible Ku70 WT and S155D expression system. Ku70 knockout MEFs were transfected with, and stably selected for, pBIG2r Tet-Off constructs of Ku70 WT and S155D. A) Levels of Ku70 expression were analyzed by western blot for both cells maintained under tetracycline control (0 h) or 24 h after the removal of tetracycline (24 h). Vinculin is included as a loading control. B) A gradual onset of Ku70 S155D expression upon the removal of tetracycline repression. Ku70 S155D is shown and the pattern for WT was similar. C) The expression of Ku70 WT and S155D was also analyzed by immunofluorescence for Ku70 with DAPI as a nuclear marker. Representative images of Ku70 expression in a subset of the the cells that have been removed from tetracycline control (24 h) but not in those maintained under tetracycline control (0 h). Images were taken with the 20x objective and scale bars represent 40 μm. D) Quantification of the the percentage of Ku70 expressing cells that also showed more than 5 γH2AX foci. This analysis was done for WT and S155D pBIG2r cells that had been removed from tetracycline control for 8 and 24 h. At least 50 cells were counted per replicate. The percentage of Ku70 expressing cells that had more than 5 γH2AX foci was greater in the Ku70 S155D pBIG2r cells than in the WT Ku70 pBIG2r cells at both the 8 and 24 h time points. Data for 2 replicates of the experiment (red and blue) are shown.

Chapter 4

Discussion

The aim of this study was to advance our understanding of the mechanisms through which Ku70 S155D functions to activate the DDR. We hypothesized that Ku70 S155D mimics phosphorylation of Ku70 in response to damage, and that Ku70 S155D is able to inhibit Aurora B leading to a sustained activation of the DDR and cell cycle arrest through activation of DDR signalling. The results suggest that the Ku70 S155D vWA domain is able to activate the DDR independent of DNA damage, and that this may be due to the inhibition of Aurora B.

4.1 Summary of results

First, the expression of Ku70 S155D does not generate endogenous DNA damage in a cell. In addition, S155A and S155D mutations within the vWA domain of Ku70 do not affect the heterodimerization of Ku70 with Ku80. We also demonstrated an association of Aurora B with WT Ku70 following IR, a condition which has previously been demonstrated to induce Ku70 S155 phosphorylation. Additionally, the association of Ku70 S155D with Aurora B *in situ* was demonstrated using PLA. Further, the Ku70 S155D vWA domain was shown to be sufficient to inhibit Aurora B in an *in vitro* kinase assay. Finally, the chemical inhibition of Aurora B in Ku70 S155D expressing cells showed no significant increase in the activation of the DDR marker γH2AX. The results of this work suggest that Ku70 S155D and phosphorylated Ku70 associate with and inhibit Aurora B, and that this inhibition is not dependent on DNA binding or heterodimerization as the Ku70 S155D vWA domain was sufficient to inhibit Aurora B. Additionally, as the inhibition of Aurora B in Ku70 S155D expressing cells did not increase DDR

markers, Ku70 S155D-dependent DDR activation may function through Aurora B inhibition.

The induction of the DNA damage response upon the expression of Ku70 S155D is a novel discovery for the function of Ku in signalling following DNA damage [91]. In order to demonstrate that this activation was not induced by DNA breaks caused by the expression of Ku70 S155D, comet assays for DNA damage were performed. The results of both the neutral and alkaline comet assays demonstrate that there is no significant difference in the level of DNA damage between WT and Ku70 S155D expressing cells. This result supports the notion that the DNA damage response activation in response to Ku70 S155D expression is not due to the creation of DNA damage but instead is an activation of signalling by the phosphomimetic mutant. This result is not surprising, as it seems unlikely that a single amino acid substitution would alter the function of Ku70 from a DNA repair protein to a DNA damage creating agent. Next, we demonstrated that the S155D and S155A mutant Ku70 proteins co-immunoprecipitate with Ku80, suggesting that the heterodimer can form. The heterodimerization of Ku70 and Ku80 has been previously been characterized to occur through the core domains of these two subunits [61]. This is consistent with our results which demonstrate that a single amino acid mutation at the Ku70 155 site within the Ku70 vWA domain does not impact heterodimerization with Ku80. Therefore the function of this heterodimer in cNHEJ repair is likely not disrputed. This result is consistent with previous data which demonstrated that a S155A/D156A double mutation does not affect the DNA repair function of Ku70 [90]. Altogether, these experiments demonstrate that the Ku70 S155D mutation does not interrupt the Ku70/Ku80 heterodimer or impact the level of endogenous DNA damage within the cell. This work is consistent with Fell and Schild-Poulter's suggestion that Ku70 S155D induces the DDR through activation of a signalling pathway [90].

Aurora B was previously identified in a screen to identify proteins which interact with Ku70 S155D [91]. This association was confirmed by Aurora B co-immunoprecipitation with Ku70 S155D *in vitro* [91]. As an extension of this work, the results in this study demonstrate that Aurora B co-immunoprecipitates with Ku70 from irradiated cells, but not from unirradiated control cells. This co-immunoprecipitation of Aurora B and Ku70 following irradiation was observed in both MEF and HeLa cells, demonstratng conservation between mamalian species. As the Ku70 S155 position has been demonstrated to be phosphorylated in response to irradiation [91], these results suggest that Aurora B associates with phosphoS155 Ku70. In order to demonstrate this association of Aurora B with Ku70 *in situ*, a proximity ligation assay was employed in cells expressing either Ku70 WT or the phosphomimetic Ku70 S155D. Aurora B was found to co-localize with Ku70 in cells expressing the S155D mutant but not with Ku70

in cells expressing Ku70 WT. This once again supports that Aurora B associates with Ku70 S155D and phosphorylated Ku70, but also demonstrates that the association occurs *in situ*. Additionally, the correspondence between the association of Aurora B with Ku70 S155D by PLA and with phosphorylated Ku70 by co-immunoprecipitation validates further use of the Ku70 S155D phosphomimetic mutant to study the role of this phosphorylation in the activation of the DDR.

In addition to demonstrating Aurora B association with Ku70 S155D, the results of *in vitro* kinase assay demonstrate that bacterially expressed Ku70 S155D vWA domain is capable of inhibiting Aurora B kinase activity. The reduction in Histone H3 phosphorylation by Aurora B in the presence of the Ku70 S155D vWA domain demonstrates an important function of this phosphomimetic mutation and therefore importance of phosphorylation. This experiment suggests that the vWA domain mediates this inhibition effect, and is sufficient to inhibit Aurora B. The sufficiency of the vWA domain in inhbition suggests that the heterodimerization and DNA binding capabilities of Ku70 are not required to inhibit Aurora B. This result is consistent with previous work by Fell *et. al.* which demonstrated that the expression of the Ku70 S155D vWA domain in cells was sufficient to induce the DDR [91]. In fact, the activation of the DDR was also observed when the Ku70 S155D vWA domain was expressed in cells with endogenous Ku70, suggesting a dominant effect [91]. Previous investigations revealed that bacterially expressed Ku70 S155D vWA domain was not sufficient to inhibit recombinant GST-Aurora B in an *in vitro* kinase assay, suggesting that the interaction is not direct (Fell and Schild-Poulter, Unpublished). This suggests that the vWA may interact with other factors associated with Aurora B. It is possible that the Ku70 S155D vWA domain interacts with an Aurora B associated factor and inhibits Aurora B directly, or that this interaction leads to alteration of a complex and indirectly decreases Aurora B kinase activity. This notion is consistent with previous research which demonstrates that INCENP and other factors are nececessary for full Aurora B kinase activity [121]. Additionally, Gohard and colleagues demonstrated that interruption of the INCENP-Aurora B interaction reduces Aurora B kinase activity [121]. Therefore, it is possible that the Ku70 S155D vWA domain interrupts such an interaction and leads to Aurora B inhibition. The inhibition of Aurora B by the Ku70 S155D vWA domain, may help explain how the Ku70 S155D vWA domain is able to activate the DDR response in both cell competent for Ku70 and cells deficient for Ku70.

The Ku70 S155D vWA inhibition of Aurora B hinted about the mechanism of Ku70 S155D-dependent activation of the DDR through the inhibition of Aurora B. Since Aurora B chemical inhibition induces a DDR, and the Ku70 S155D vWA domain inhibits Aurora B and induces a

DDR, we suggested that Ku70 S155D, or phosphoS155 Ku70, induces DDR activation through Aurora B inhibition. However, the sequential effect of Ku70 S155D expression leading to Aurora B inhibition which in turn causes the DDR had not been investigated. This led us to test for an additive effect of Ku70 S155D expression and the inhibition of Aurora B. Consistent with results that were previously demonstrated by Fell *et. al.* (2016), the treatment of WT Ku70 MEFs with an Aurora B inhibitor resulted in the activation of the DDR, as characterized by the increase in the number of cells with more than 5 γH2AX foci. A similar activation of the DDR, and therefore the presence of DDR markers, is also seen in untreated Ku70 S155D expressing MEFs. However, the treatment of Ku70 S155D expressing MEFs with an Aurora B inhibitor did not trigger an increase in γH2AX foci relative to untreated Ku70 S155D cells. There are two possible explanations for this result: First, Aurora B is already inhibited in Ku70 S155D MEFs, so the addition of the Aurora B inhibitor is redundant and does not increase the activation of the DDR. This explanation is consistent with previous work by Fell *et. al.* (2016) which demonstrated that Aurora B immunoprecipitated from Ku70 S155D MEFs is inhibited in its kinase activity. However, a second explanation of this result that cannot currently be ruled out is that cell expressing Ku70 S155D already have reached a maximal threshold of γH2AX activation. Therefore, even though the Aurora B inhibitor may functionally inhibit Aurora B and activate the DDR, this activation is masked by the DDR activated by Ku70 S155D. These results suggest that DDR activation through Ku70 S155D expression occurs at least in part from Aurora B inhibition, but further experimentation will be needed to confirm this.

Finally, a Tet-off system for Ku70 WT and S155D expression was established. The removal of tetracycline from cells selected to have integrated Ku70 S155D or WT pBIG2r plasmids triggers the induction of Ku70 expression. The expression of Ku70 WT and S155D in these cells was demonstrated by western blot and immunofluorescence assay. In both western blot and immunofluorescence analysis, the expression of the Ku70 S155D appeared to be lower than its WT counterpart. This could be due to a lower per cell expression, but immunofluorescence assay demonstrates a lower percentage of cells are expressing Ku70 S155D than in the WT. The expression of Ku70 S155D is unfavourable to the cells, which may partially explain the lower proportion of Ku70 S155D expressing cells when compared to the corresponding WT Ku70 expression. However, WT Ku70 is also not expressed in all cells following tetracycline removal. It is possible that the expression in these cells may take longer and therefore was not detected at the 24 h time point and that later analysis would be needed to demonstrate a larger proportion of WT Ku70 expressing cells. Alternatively, it is possible that these cells do not contain the WT Ku70 pBIG2r construct and have developed or maintained resistance to hygromycin selection which allowed for their survival. Future experiments to address this issue

could include testing MEF sensitivity to hygromycin and increasing the hygromycin selection concentration following pBIG2r construct transfection. The establishment of this system will be important for future work into the time line for and mechanism of Ku70 S155D inhibition of Aurora B leading to activation of cell cycle checkpoints and the DDR (See Future Work).

4.2 Significance of the Ku70 S155D association with and inhibition of Aurora B

The Ku70 S155 site has not been previously identified as a site for phosphorylation in proteomic studies [122]. However, this may be due to low level phosphorylation of this position in response to DNA damage [91].

Our proposed model is that following DNA damage, Ku initiates repair through the recruitment of the repair complex. In the case of successful repair, Ku70 is not phosphorylated at the S155 amino acid. In the case of repair no Aurora B inhibition occurs. Therefore, signalling to the DDR is hindered. We propose that in the event of overwhelming DNA damage, Ku70 is recruited to the break but DNA repair cannot be completed. This may occur because Ku is much more abundant than other members of the cNHEJ. Therefore, in the case of overwhelming DNA damage, Ku would bind at all DNA breaks but is not able to recruit a functional repair complex to every DNA break. Alternatively, repair may be slowed by the complexity of the DNA break, and therefore need increased time for processing. We suggest that in this case Ku becomes phosphorylated and interacts with the Aurora B complex resulting in Aurora B inhibition (Figure 4.1). The inhibition of Aurora B is associated with a corresponding increase in DDR activation and activation of the cell cycle checkpoints. This hypothetical model helps to explain the low levels of Ku70 S155 phosphorylation as well as the activation of the DDR response seen upon the expression of Ku70 S155D, which is a stronger and sustained mimic of the equivalent endogenous phosphorylation.

In addition to demonstrating an interaction of Ku70 S155D and Aurora B, previous work showed that the expression of Ku70 S155D led to the inhibition of Aurora B, demonstrated using an *in vitro* kinase assay [91]. This work also investigated the effect of FLAG-Tagged Ku70 WT and S155D vWA domain expression in Ku70 knockout MEFs and in human IMR-90 cells which have endogenous Ku70. In both the knockout and endogenous human Ku backgrounds, the expression of the Ku70 S155D vWA domain led to decreased proliferation and increased

p21 levels relative to WT Ku70 vWA domain expression [91]. The work in this thesis expands upon this by demonstrating that the Ku70 S155D vWA domain alone is sufficient to inhibit Aurora B *in vitro*, which helps to explain the dominant effect of the Ku70 S155D vWA domain in IMR90 cells. This Ku70 S155D vWA-dependent inhibition suggests that the phosphorylation of the S155 site can induce a signalling response which inhibits Aurora B and activates the DDR, independent of DNA binding and heterodimerization with Ku80. The role of Aurora B in the DDR remains to be characterized, but the effects of Aurora B inhibitors in this and other studies, support that inhibition leads to activation of DDR signalling [91, 95, 109, 110]. However, we still cannot rule out that the DDR response of Ku70 S155D expression is activated by mechanisms distinct from Aurora B inhibition.

4.3 Aurora B and the DDR

Aurora B has been previously linked to DDR signalling through interactions with proteins including: PARP1 and ATM [55, 112]. The DDR-dependent activation of PARP1 was demonstrated to poly(ADP- ribosyl)ate Aurora B, which results in inhibition of Aurora B kinase activity [112]. This study additionally demonstrated that induction of DNA damage (through irradiation or H_2O_2 treatment) was associated with lower levels of phosphorylated Histone H3 while levels of Aurora B remain constant [112]. The decrease in phosphorylation of Histone H3 was abrogated in cells deficient for PARP1, which suggests that in response to DNA damage, Aurora B kinase activity is inhibited through PARP1 activity. Aurora B kinase activity was also previously shown to be inhibited through ATM-dependent phosphorylation of I-2, which removes inhibition of and therefore activates PP1 [55]. The inhibition of Aurora B in this manner was once again associated with decreased levels of Histone H3 phosphorylation but also with the induction of the G2/M cell cycle checkpoint [55]. This result was corroborated by similar research which showed Aurora B inhibition in the presence of active PP1 [123]. The results of the discussed studies parallel those in this thesis, and demonstrate a role for Aurora B in DDR signalling.

4.4 Ku70 and the DDR

In concurrence with the work in this thesis, Tomimatsu and colleagues have also documented a role for Ku in the DDR, outside of its repair function [48]. These authors were interested in the

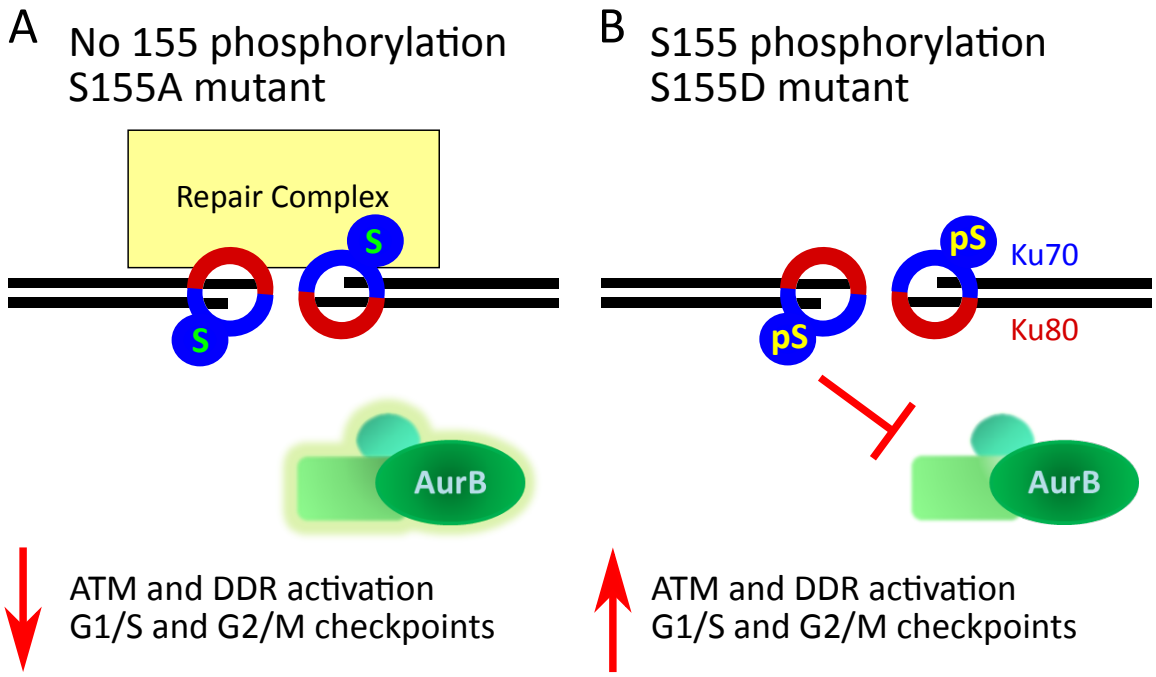

Figure 4.1: Revised model for the cells response to DNA damage through Ku70 phosphorylation. Upon DNA DSB induction Ku70 is recruited to the break. A) In the case of successful repair we propose that Ku70 S155 does not become phosphorylated and therefore Aurora B remains active. This means that there is no additional DDR activation or cell cycle arrest. This is also the case when Ku70 S155A, which cannot be phosphorylated, is expressed. B) We propose that in the event of overwhelming or complex damage, DNA repair is inefficient or delayed. In this case Ku70 S155 becomes phosphorylated and interacts with the Aurora B complex, leading to Aurora B inhibition. This leads to increased DDR activation and cell cycle arrest. This also occurs when the phosphomimetic Ku70 S155D is expressed.

possible modulation of ATM and ATR kinases by the Ku heterodimer [48]. They provide evidence that the Ku heterodimer modulates ATM-dependent activation of ATR and that activated ATR acts to phosphorylate p53 [48]. The phosphorylation of p53 by ATM and ATR is a key step in the activation of the DDR, specifically in the activation of cell cycle checkpoints and apoptosis [48]. The authors additionally demonstrate that in both Ku70- and Ku80-deficient cells, ATR is activated in a ATM-independent way, and that this type of activation leads to the irregular persistence of p53 phosphorylation following IR [48]. The overall conclusion of this study is that the Ku heterodimer is necessary for the ATM-dependent activation of ATR. The work by Tomimatsu and colleagues demonstrates, as this work does, that Ku at DSBs has a function beyond the recruitment of repair factors and into the modulation of DDR signalling pathways.

4.5 Ku70 S155, the DDR, and cancer

A number of members of the cNHEJ pathway have been associated with cancer and aging [124]. Theoretically, the cNHEJ can counteract the efficacy of cancer treatments such as chemotherapy and radiation therapy which induce DSBs to target cancer cells. However, the cNHEJ, like most pathways in cancer cells, becomes deregulated and these treatments target the components of this pathway in cancer cells [11, 13, 124]. Therefore drugs targeting members of the cNHEJ, including inhibitors of Ku protein-protein and protein-DNA interactions, are potential sensitizers to chemotheraputic and radiation treatments [124].

Ku is frequently deregulated for both activity and expression in tumour samples [125, 126, 127, 128]. The Ku70 S155 site specifically has not been identified as a site of mutation in cancer by the Catalogue of Somatic Mutations in Cancer (COSMIC). The absence of a Ku70 S155D mutation in cancer is not surprising, as the expression of such a Ku70 mutant would activate the DDR and cause cell cycle arrest, features that are unfavourable to cancer progression. However, the expression of a S155A Ku70, which could not be phosphorylated and has an increased growth rate relative to WT Ku70 MEFs, would be a more likely mutation favouring cancer development. Although such a mutation has also not been demonstrated, a D156N mutation was identified in a lung carcinoma sample (Figure 4.2) [129]. This aspartic acid to asparagine amino acid change represents a change from a negatively charged side group to an uncharged but polar side chain of similar size and structure. This alteration of charge could interrupt the phosphorylation of the S155 site. Specifically, the SXXQ (a.a. 155-158) consensus sequence has been identified as a consensus sequence for kinases such as ATM and

DNA-PK [122]. The charge alteration in this region may affect the ability of the kinase responsible for phosphorylation to recognize the sequence and phosphorylate Ku70. Therefore, the D156N mutation in the lung carcinoma sample may suppress the Ku70 S155 phosphorylation-dependent activation of the DDR that has been described in this work.

Additionally, there are three other mutations recorded in the COSMIC database that occur just a few amino acids before the S155 site (Figure 4.2). These V149I, A151V, and L153F mutations are not directly part of the predicted SXXQ consensus sequence for Ku70 phosphorylation, but it is still possible that they could alter the probability of the S155 becoming phosphorylated because of their proximity to the site.

While the S155D and S155A mutations of interest in this work have not been identified in cancer, they may still have a role to play in our understanding of, and maybe even in treatment of cancer. For example, the ability of the Ku70 S155D vWA domain to inhibit Aurora B *in vitro* and to have a dominant effect over endogenous Ku70 in the activation of the DDR are promising results. They suggest that the expression of a Ku70 S155D peptide or the manipulation of the endogenous Ku70 S155 site could be used to activate the DDR in cancer cells and cause cell cycle arrest or even apoptosis. This treatment could be use in combination with other compounds to therapeutically suppress tumour growth.

4.6 Future directions

While this research has identified a novel role for the phosphorylation of the Ku70 vWA domain in inhibiting Aurora B and activating the DDR, there is still much to be characterized with regards to this pathway.

A first major question to be addressed in the future is: What phosphorylates Ku70 following the induction of DNA DSBs? This question has been of ongoing interest but has proven difficult to determine without a specific and functional phospho-S155 Ku70 antibody. The DDR is a complex network of kinases, and therefore there are many candidate kinases which could be responsible for Ku70 S155 phosphorylation. However, the S155 site is contained in a SDVQ sequence which matches a loose SXXQ consensus sequence which has been demonstrated to be phosphorylated by ATM and DNA-PK [122]. These two kinases are therefore likely candidates for Ku70 S155 phosphorylation. With a p155 Ku70 specific antibody, the phosphorylation of the S155 Ku70 site could be monitored and quantified following induction of DNA damage

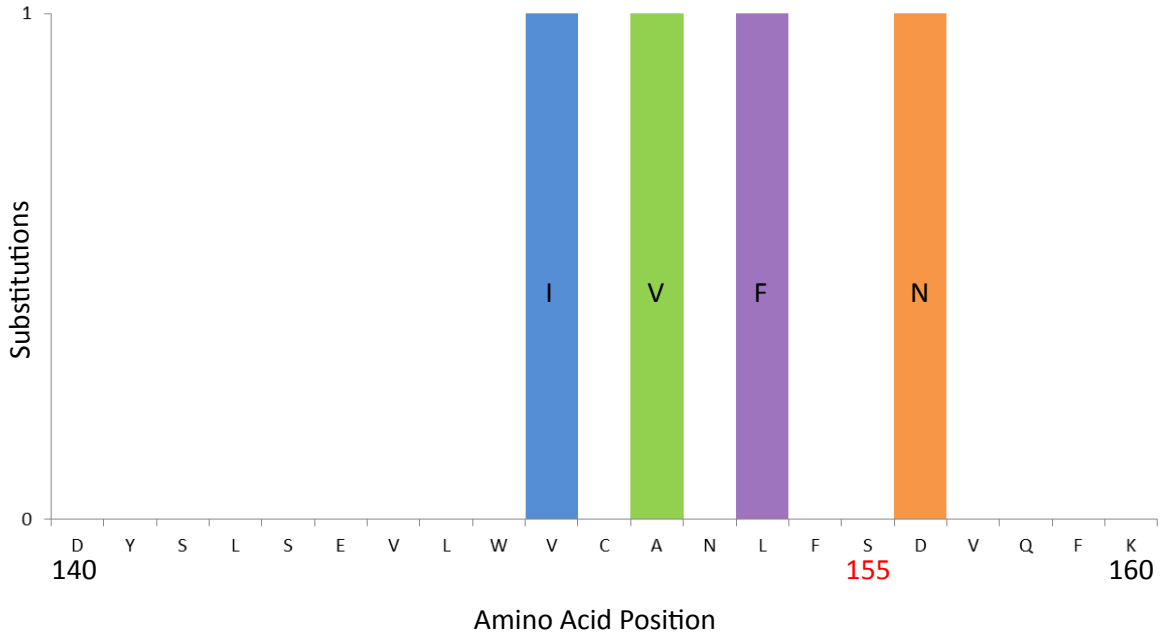

Figure 4.2: Substitution mutations near the S155 site recorded in cancers by the COSMIC database. There is a cluster of mutations proximal to the S155 amino acid of the Ku70 vWA domain which have been identified within tumour samples. Mutations between amino acids 140-160 of the Ku70 vWA domain as documented in the COSMIC database. This image was derived from information in the COSMIC database [129].

in the presence of an ATM or DNA-PK inhibitor, or in competent/deficient cell line pairs for these kinases. Additionally, to specifically determine the kinase responsible, these experiments could be paired with *in vitro* assays for Ku70 S155 phosphorylation.

In addition to possibly being the kinase responsible for Ku70 phosphorylation, the role for ATM in the Ku70 S155D-dependent inhibition of Aurora B and activation of the DDR is of interest. Previous work demonstrated that ATM is phosphorylated at S1981 in response to Ku70 S155D expression [91]. This phosphorylation is well documented as a key event in the activation of ATM, which in turn acts as the apex kinase in the DDR [46, 49]. The DDR is an extensive network, so although possible that Ku70 phosphorylation (or Ku70 S155D expression) activates an alternate pathway with the same endpoint and markers, it it likely that this signalling converges into the ATM dependent signalling pathway. It would therefore be interesting to further study this work in an ATM competent/deficient cell line pair in order to determine if the DDR activated by Ku70 S155D expression is dependent on ATM.

A second major gap is the lack of understanding of how Ku70 inhibits Aurora B and induces DDR signalling. Future work could investigate other proteins that associate with Ku70 S155D and Aurora B to determine mediators of the interaction and inhibition. One method to identify interactors is BioID, a method which uses a promiscuous biotin ligase-bait fusion protein, which will biotinylate proteins that exist in proximity to the bait protein [130]. In the future, Ku70 WT-biotin ligase and Ku70 S155D-biotin ligase fusion protein could be generated and independently infected into $Ku70^{-/-}$ MEFs. In the cell the promiscuous biotin ligase would biotinylate proteins in proximity to the Ku fusions. A pull down for biotinylated proteins would enrich for proteins that are tagged with biotin. These proteins could then be identified through mass spectrometry and the list of proteins associated with Ku70 WT and S155D compared. Proteins that preferentially associate with Ku70 S155D could further be validated for their role in the Ku70 S155D-dependent inhibition of Aurora B and activation of the DDR. Likely candidates include other members of the chromosomal passenger complex or key kinases of the DDR. It was previously demonstrated that ATM and ATF2 are phosphorylated, and therefore activated in Ku70 S155D cells [90, 91]. Both of these proteins signal for cell cycle arrest through the DDR. Additionally, p21, a key effector of the DDR, was demonstrated to be upregulated [91]. These results suggest that ATM and ATF2 regulation play a role in Ku70 S155D dependent activation of the DDR, and that they may therefore be identified in a BioID screen. In further studies, the mechanism of the Aurora B inhibition leading to activation of the DDR through associated proteins could be studied using a similar system. Knowledge of other proteins which interact with Ku70 S155D and Aurora B may be vital to developing an

understanding of the mechanism of Aurora B inhibition by phosphoS155 Ku70 and how this leads to DDR activation.

Another avenue for future research into the mechanism of DDR activation through Ku70 S155D expression is determining the preliminary response to Ku70 S155D expression. Fell and colleagues (2016), demonstrated that both a DNA damage response and cell cycle arrest are induced upon Ku70 S155D expression [91]. However, the activation of the DDR leads to cell cycle arrest, and cell cycle arrest can lead to activation of the DDR [131, 132]. Therefore, it remains unclear whether Ku70 S155D expression first leads to DDR or cell cycle arrest. Future studies could use the Tet-off Ku70 WT and S155D expression system developed in this thesis to study the onset of the DDR and cell cycle arrest upon expression of Ku70 WT or S155D. Specifically, this system in combination with cell cycle synchronization could be used to determine whether the DDR or cell cycle arrest response of Ku70 S155D expression occurs as the primary effect. Tet-off Ku70 WT and S155D cells chemically arrested in the G1 stage could be removed from tetracycline to allow for Ku70 WT or S155D expression. These cells could then be analyzed for DNA damage response markers or released from chemically-induced cell cycle arrest and analyzed for Ku70 S155D-induced cell cycle arrest and DNA damage markers at time points following release. Such an experiment would aim to determine if Ku70 S155D-dependent DNA damage markers appear, then cell cycle arrest occurs, or if Ku70 S155D-dependent cell cycle arrest occurs, then the DDR markers appear, thereby determining the primary effect of Ku70 S155D expression and Ku70 phosphorylation.

A final interesting avenue for future research is to investigate the ability of the Ku70 S155 site phosphorylation state to regulate cell cycle arrest. In the future, the expression of a Ku70 S155D peptide or the manipulation of the endogenous Ku70 S155 site could be used as a therapeutic to induce cell cycle arrest and apoptosis in cancer cells.

4.7 Conclusions

The main goal of this work was to determine how phosphorylated Ku70, through experimentation using the phosphomimetic Ku70 S155D, is able to inhibit Aurora B and mediate the DDR and cell cycle arrest. Work in this thesis demonstrated that substitutions at the Ku70 S155 site do not affect heterodimerization or the endogenous cellular levels of DNA damage. Additionally, this work characterized the association of Aurora B with phosphorylated Ku70 and Ku70 S155D, and the role of Ku70 S155D in the inhibition of Aurora B. Specifically, the

Ku70 S155D vWA domain is sufficient to inhibit the activity of immunoprecipitated Aurora B. Experiments involving Aurora B inhibition in Ku70 S155D expressing cells potentially suggest that Aurora B inhibition by Ku70 S155D leads to the the activation of the DDR. Finally, in addition to developing our understanding of the Ku70 S155 site role in Aurora B inhibition and DDR activation, this work has created systems and laid groundwork that will allow for future research to also further our understanding of this novel signalling pathway.

Chapter 5

Bibliography

[1] Canadian Cancer Societys Advisory Committee on Cancer Statistics. *Canadian Cancer Statistics.* (2016).

[2] Hanahan, D. & Weinberg, R. A. The hallmarks of cancer. *Cell* **100**, 57–70 (2000).

[3] Hanahan, D. & Weinberg, R. A. Hallmarks of cancer: the next generation. *Cell* **144**, 646–674 (2011).

[4] Deriano, L. & Roth, D. B. Modernizing the nonhomologous end-joining repertoire: alternative and classical NHEJ share the stage. *Annual review of genetics* **47**, 433–55 (2013).

[5] Sedelnikova, O. A. *et al.* Role of oxidatively induced {DNA} lesions in human pathogenesis. *Mutation Research/Reviews in Mutation Research* **704**, 152 – 159 (2010).

[6] Durdíková, K. & Chovanec, M. Regulation of non-homologous end joining via post-translational modifications of components of the ligation step. *Current Genetics* 1–15 (2016).

[7] Ciccia, A. & Elledge, S. J. The DNA damage response: making it safe to play with knives. *Mol. Cell* **40**, 179–204 (2010).

[8] Vilenchik, M. M. & Knudson, A. G. Endogenous DNA double-strand breaks: production, fidelity of repair, and induction of cancer. *Proc. Natl. Acad. Sci. U.S.A.* **100**, 12871–12876 (2003).

[9] Surova, O. & Zhivotovsky, B. Various modes of cell death induced by DNA damage. *Oncogene* **32**, 3789–3797 (2013).

[10] Warmerdam, D. O. & Kanaar, R. Dealing with DNA damage: Relationships between checkpoint and repair pathways. *Mutation Research - Reviews in Mutation Research* **704**, 2–11 (2010).

[11] Curtin, N. J. DNA repair dysregulation from cancer driver to therapeutic target. *Nature Reviews Cancer* **12**, 801–817 (2012).

[12] Hoeijmakers, J. H. J. DNA damage, aging, and cancer. *The New England journal of medicine* **361**, 1475–85 (2009).

[13] Hosoya, N. & Miyagawa, K. Targeting DNA damage response in cancer therapy. *Cancer Science* **105**, 370–388 (2014).

[14] Chapman, J. R., Taylor, M. R. G. & Boulton, S. J. Review Playing the End Game : DNA Double-Strand Break Repair Pathway Choice. *MOLCEL* **47**, 497–510 (2012).

[15] Takata, M. *et al.* Homologous recombination and non-homologous end-joining pathways of DNA double-strand break repair have overlapping roles in the maintenance of chromosomal integrity in vertebrate cells. *EMBO J.* **17**, 5497–5508 (1998).

[16] Cook, R. *et al.* Direct Involvement of Retinoblastoma Family Proteins in DNA Repair by Non-homologous End-Joining. *Cell Reports* **10**, 2006–2018 (2015).

[17] San Filippo, J., Sung, P. & Klein, H. Mechanism of eukaryotic homologous recombination. *Annu. Rev. Biochem.* **77**, 229–257 (2008).

[18] Rothkamm, K. & Lobrich, M. Evidence for a lack of DNA double-strand break repair in human cells exposed to very low x-ray doses. *Proc. Natl. Acad. Sci. U.S.A.* **100**, 5057–5062 (2003).

[19] Mahaney, B. L., Meek, K. & Lees-Miller, S. P. Repair of ionizing radiation-induced DNA double-strand breaks by non-homologous end-joining. *Biochem. J.* **417**, 639–650 (2009).

[20] Andres, S. N. *et al.* A human XRCC4-XLF complex bridges DNA. *Nucleic Acids Res.* **40**, 1868–1878 (2012).

[21] Chang, H. H. & Lieber, M. R. Structure-Specific nuclease activities of Artemis and the Artemis: DNA-PKcs complex. *Nucleic Acids Res.* **44**, 4991–4997 (2016).

[22] Woodbine, L., Brunton, H., Goodarzi, A. A., Shibata, A. & Jeggo, P. A. Endogenously induced DNA double strand breaks arise in heterochromatic DNA regions and require ataxia telangiectasia mutated and Artemis for their repair. *Nucleic Acids Res.* **39**, 6986–6997 (2011).

[23] Chappell, C., Hanakahi, L. A., Karimi-Busheri, F., Weinfeld, M. & West, S. C. Involvement of human polynucleotide kinase in double-strand break repair by non-homologous end joining. *EMBO J.* **21**, 2827–2832 (2002).

[24] Strande, N., Roberts, S. A., Oh, S., Hendrickson, E. A. & Ramsden, D. A. Specificity of the dRP/AP lyase of Ku promotes nonhomologous end joining (NHEJ) fidelity at damaged ends. *J. Biol. Chem.* **287**, 13686–13693 (2012).

[25] Postow, L. *et al.* Ku80 removal from DNA through double strand break-induced ubiquitylation. *J. Cell Biol.* **182**, 467–479 (2008).

[26] Postow, L. Destroying the ring: Freeing DNA from Ku with ubiquitin. *FEBS Lett.* **585**, 2876–2882 (2011).

[27] Lieber, M. R. The mechanism of double-strand DNA break repair by the nonhomologous DNA end-joining pathway. *Annu. Rev. Biochem.* **79**, 181–211 (2010).

[28] Nussenzweig, A. *et al.* Requirement for Ku80 in growth and immunoglobulin V(D)J recombination. *Nature* **382**, 551–555 (1996).

[29] Dai, Y. *et al.* Nonhomologous end joining and V(D)J recombination require an additional factor. *Proc. Natl. Acad. Sci. U.S.A.* **100**, 2462–2467 (2003).

[30] Soulas-Sprauel, P. *et al.* V(D)J and immunoglobulin class switch recombinations: a paradigm to study the regulation of DNA end-joining. *Oncogene* **26**, 7780–7791 (2007).

[31] Dueva, R. & Iliakis, G. Alternative pathways of non-homologous end joining (nhej) in genomic instability and cancer. *Translational Cancer Research* **2** (2013).

[32] Frit, P., Barboule, N., Yuan, Y., Gomez, D. & Calsou, P. Alternative end-joining pathway(s): bricolage at DNA breaks. *DNA Repair (Amst.)* **17**, 81–97 (2014).

[33] Fell, V. L. & Schild-Poulter, C. The Ku heterodimer: function in DNA repair and beyond. *Mutat Res Rev Mutat Res* **763**, 15–29 (2015).

[34] Bunting, S. F. & Nussenzweig, A. End-joining, translocations and cancer. *Nat. Rev. Cancer* **13**, 443–454 (2013).

[35] Simsek, D. & Jasin, M. Alternative end-joining is suppressed by the canonical NHEJ component Xrcc4-ligase IV during chromosomal translocation formation. *Nat. Struct. Mol. Biol.* **17**, 410–416 (2010).

[36] Clouaire, T. & Legube, G. DNA double strand break repair pathway choice: a chromatin based decision? *Nucleus* **6**, 107–113 (2015).

[37] Kakarougkas, A. & Jeggo, P. A. DNA DSB repair pathway choice: an orchestrated handover mechanism. *Br J Radiol* **87**, 20130685 (2014).

[38] Fattah, F. *et al.* Ku regulates the non-homologous end joining pathway choice of DNA double-strand break repair in human somatic cells. *PLoS Genet.* **6**, e1000855 (2010).

[39] Pierce, A. J., Hu, P., Han, M., Ellis, N. & Jasin, M. Ku DNA end-binding protein modulates homologous repair of double-strand breaks in mammalian cells. *Genes Dev.* **15**, 3237–3242 (2001).

[40] Langerak, P., Mejia-Ramirez, E., Limbo, O. & Russell, P. Release of Ku and MRN from DNA ends by Mre11 nuclease activity and Ctp1 is required for homologous recombination repair of double-strand breaks. *PLoS Genet.* **7**, e1002271 (2011).

[41] Finn, K., Lowndes, N. F. & Grenon, M. Eukaryotic DNA damage checkpoint activation in response to double-strand breaks. *Cellular and Molecular Life Sciences* **69**, 1447–1473 (2012).

[42] Lavin, M. F. & Kozlov, S. ATM activation and DNA damage response. *Cell Cycle* **6**, 931–942 (2007).

[43] Polo, S. & Jackson, S. Dynamics of DNA damage response proteins at DNA breaks: a focus on protein modifications. *Genes & development* **25**, 409–33 (2011).

[44] Giglia-Mari, G., Zotter, A. & Vermeulen, W. DNA damage response. *Cold Spring Harbor Perspectives in Biology* **3**, 1–19 (2011).

[45] Fumagalli, M., Rossiello, F., Mondello, C. & d'Adda di Fagagna, F. Stable cellular senescence is associated with persistent DDR activation. *PLoS ONE* **9**, e110969 (2014).

[46] Bensimon, A., Aebersold, R. & Shiloh, Y. Beyond ATM: The protein kinase landscape of the DNA damage response. *FEBS Letters* **585**, 1625–1639 (2011).

[47] Matsuoka, S. *et al.* ATM and ATR substrate analysis reveals extensive protein networks responsive to DNA damage. *Science* **316**, 1160–1166 (2007).

[48] Tomimatsu, N. *et al.* Ku70/80 modulates ATM and ATR signaling pathways in response to DNA double strand breaks. *Journal of Biological Chemistry* **282**, 10138–10145 (2007).

[49] Sulli, G., Di Micco, R. & d'Adda di Fagagna, F. Crosstalk between chromatin state and DNA damage response in cellular senescence and cancer. *Nature Reviews Cancer* **12**, 709–720 (2012).

[50] Falck, J., Coates, J. & Jackson, S. P. Conserved modes of recruitment of ATM, ATR and DNA-PKcs to sites of DNA damage. *Nature* **434**, 605–611 (2005).

[51] Yoshiyama, K. O., Sakaguchi, K. & Kimura, S. DNA Damage Response in Plants: Conserved and Variable Response Compared to Animals. *Biology* **2**, 1338–1356 (2013).

[52] Batchelor, E., Loewer, A. & Lahav, G. The ups and downs of p53: understanding protein dynamics in single cells. *Nat. Rev. Cancer* **9**, 371–377 (2009).

[53] Küntziger, T., Landsverk, H. B., Collas, P. & Syljuåsen, R. G. Protein phosphatase 1 regulators in DNA damage signaling. *Cell Cycle* **10**, 1356–1362 (2011).

[54] Peng, A., Lewellyn, A. L., Schiemann, W. P. & Maller, J. L. Repo-Man Controls a Protein Phosphatase 1-Dependent Threshold for DNA Damage Checkpoint Activation. *Current Biology* **20**, 387–396 (2010).

[55] Tang, X. *et al.* A novel ATM-dependent pathway regulates protein phosphatase 1 in response to DNA damage. *Molecular and cellular biology* **28**, 2559–66 (2008).

[56] Downs, J. A. & Jackson, S. P. A means to a DNA end: the many roles of Ku. *Nat. Rev. Mol. Cell Biol.* **5**, 367–378 (2004).

[57] Gu, Y. *et al.* Growth retardation and leaky SCID phenotype of Ku70-deficient mice. *Immunity* **7**, 653–665 (1997).

[58] Li, H., Vogel, H., Holcomb, V. B., Gu, Y. & Hasty, P. Deletion of Ku70, Ku80, or both causes early aging without substantially increased cancer. *Mol. Cell. Biol.* **27**, 8205–8214 (2007).

[59] Griffith, A. J., Blier, P. R., Mimori, T. & Hardin, J. A. Ku polypeptides synthesized in vitro assemble into complexes which recognize ends of double-stranded DNA. *J. Biol. Chem.* **267**, 331–338 (1992).

[60] Koike, M., Yutoku, Y. & Koike, A. Nuclear localization of mouse Ku70 in interphase cells and focus formation of mouse Ku70 at DNA damage sites immediately after irradiation. *The Journal of veterinary medical science / the Japanese Society of Veterinary Science* **77**, 1137–42 (2015).

[61] Walker, J. R., Corpina, R. A. & Goldberg, J. Structure of the Ku heterodimer bound to DNA and its implications for double-strand break repair. *Nature* **412**, 607–614 (2001).

[62] Rivera-Calzada, A., Spagnolo, L., Pearl, L. H. & Llorca, O. Structural model of full-length human Ku70-Ku80 heterodimer and its recognition of DNA and DNA-PKcs. *EMBO Rep.* **8**, 56–62 (2007).

[63] Aravind, L. & Koonin, E. V. SAP - a putative DNA-binding motif involved in chromosomal organization. *Trends Biochem. Sci.* **25**, 112–114 (2000).

[64] Whittaker, C. A. & Hynes, R. O. Distribution and evolution of von Willebrand/integrin A domains: widely dispersed domains with roles in cell adhesion and elsewhere. *Mol. Biol. Cell* **13**, 3369–3387 (2002).

[65] Downs, J. A. & Jackson, S. P. Involvement of DNA end-binding protein Ku in Ty element retrotransposition. *Mol. Cell. Biol.* **19**, 6260–6268 (1999).

[66] Frost, J. R. *et al.* The interaction of adenovirus E1A with the mammalian protein Ku70/XRCC6. *Virology* **500**, 11–21 (2017).

[67] Wang, B. *et al.* Role of Ku70 in deubiquitination of Mcl-1 and suppression of apoptosis. *Cell death and differentiation* **21**, 1160–9 (2014).

[68] Cohen, H. Y. *et al.* Acetylation of the C terminus of Ku70 by CBP and PCAF controls Bax-mediated apoptosis. *Mol. Cell* **13**, 627–638 (2004).

[69] Amsel, A. D., Rathaus, M., Kronman, N. & Cohen, H. Y. Regulation of the proapoptotic factor Bax by Ku70-dependent deubiquitylation. *Proc. Natl. Acad. Sci. U.S.A.* **105**, 5117–5122 (2008).

[70] Wang, Y., Ghosh, G. & Hendrickson, E. A. Ku86 represses lethal telomere deletion events in human somatic cells. *Proc. Natl. Acad. Sci. U.S.A.* **106**, 12430–12435 (2009).

[71] Li, G., Nelsen, C. & Hendrickson, E. A. Ku86 is essential in human somatic cells. *Proc. Natl. Acad. Sci. U.S.A.* **99**, 832–837 (2002).

[72] d'Adda di Fagagna, F. *et al.* Effects of DNA nonhomologous end-joining factors on telomere length and chromosomal stability in mammalian cells. *Curr. Biol.* **11**, 1192–1196 (2001).

[73] Li, G., Nelsen, C. & Hendrickson, E. A. Ku86 is essential in human somatic cells. *Proc. Natl. Acad. Sci. U.S.A.* **99**, 832–837 (2002).

[74] Gravel, S., Larrivee, M., Labrecque, P. & Wellinger, R. J. Yeast Ku as a regulator of chromosomal DNA end structure. *Science* **280**, 741–744 (1998).

[75] Nandakumar, J. & Cech, T. R. Finding the end: recruitment of telomerase to telomeres. *Nat. Rev. Mol. Cell Biol.* **14**, 69–82 (2013).

[76] De Sena-Tomas, C. *et al.* Fungal Ku prevents permanent cell cycle arrest by suppressing DNA damage signaling at telomeres. *Nucleic Acids Research* **43**, 2138–2151 (2015).

[77] Chen, C. S. *et al.* Histone deacetylase inhibitors sensitize prostate cancer cells to agents that produce DNA double-strand breaks by targeting Ku70 acetylation. *Cancer Res.* **67**, 5318–5327 (2007).

[78] Subramanian, C., Hada, M., Opipari, A. W., Castle, V. P. & Kwok, R. P. CREB-binding protein regulates Ku70 acetylation in response to ionization radiation in neuroblastoma. *Mol. Cancer Res.* **11**, 173–181 (2013).

[79] Hada, M., Subramanian, C., Andrews, P. C. & Kwok, R. P. Cytosolic Ku70 regulates Bax-mediated cell death. *Tumour Biol.* **37**, 13903–13914 (2016).

[80] Brown, J. S. *et al.* Neddylation promotes ubiquitylation and release of Ku from DNA-damage sites. *Cell Rep* **11**, 704–714 (2015).

[81] Mukherjee, S., Chakraborty, P. & Saha, P. Phosphorylation of Ku70 subunit by cell cycle kinases modulates the replication related function of Ku heterodimer. *Nucleic Acids Research* **44**, gkw622 (2016).

[82] Lee, K. J. *et al.* Phosphorylation of Ku dictates DNA double-strand break (DSB) repair pathway choice in S phase. *Nucleic Acids Res.* **44**, 1732–1745 (2016).

[83] Chan, D. W., Ye, R., Veillette, C. J. & Lees-Miller, S. P. DNA-dependent protein kinase phosphorylation sites in Ku 70/80 heterodimer. *Biochemistry* **38**, 1819–1828 (1999).

[84] Douglas, P., Gupta, S., Morrice, N., Meek, K. & Lees-Miller, S. P. DNA-PK-dependent phosphorylation of Ku70/80 is not required for non-homologous end joining. *DNA Repair* **4**, 1006–1018 (2005).

[85] Jin, S. & Weaver, D. T. Double-strand break repair by Ku70 requires heterodimerization with Ku80 and DNA binding functions. *EMBO J.* **16**, 6874–6885 (1997).

[86] Lee, K. J. *et al.* Phosphorylation of Ku dictates DNA double-strand break (DSB) repair pathway choice in S phase. *Nucleic Acids Research* **44**, 1732–1745 (2015).

[87] Liu, J., Naegele, J. R. & Lin, S. L. The DNA-PK catalytic subunit regulates Bax-mediated excitotoxic cell death by Ku70 phosphorylation. *Brain Research* **1296**, 164–175 (2009).

[88] Morii, M. *et al.* Src Acts as an Effector for Ku70-dependent Suppression of Apoptosis through Phosphorylation of Ku70 at Tyr-530. *J. Biol. Chem.* (2016).

[89] Bouley, J. *et al.* A new phosphorylated form of Ku70 identified in resistant leukemic cells confers fast but unfaithful DNA repair in cancer cell lines. *Oncotarget* **6**, 27980–28000 (2015).

[90] Fell, V. L. & Schild-Poulter, C. Ku Regulates Signaling to DNA Damage Response Pathways through the Ku70 von Willebrand A Domain. *Molecular and Cellular Biology* **32**, 76–87 (2012).

[91] Fell, V. L. *et al.* Ku70 Serine 155 mediates Aurora B inhibition and activation of the DNA damage response. *Sci Rep* **6**, 37194 (2016).

[92] Carmena, M., Ruchaud, S. & Earnshaw, W. C. Making the Auroras glow: regulation of Aurora A and B kinase function by interacting proteins. *Current Opinion in Cell Biology* **21**, 796–805 (2009).

[93] Vader, G. & Lens, S. M. The Aurora kinase family in cell division and cancer. *Biochimica et biophysica acta* **1786**, 60–72 (2008).

[94] Fu, J., Bian, M., Jiang, Q. & Zhang, C. Roles of Aurora kinases in mitosis and tumorigenesis. *Molecular cancer research : MCR* **5**, 1–10 (2007).

[95] Harrington, E. A. *et al.* VX-680, a potent and selective small-molecule inhibitor of the Aurora kinases, suppresses tumor growth in vivo. *Nat. Med.* **10**, 262–267 (2004).

[96] Lok, W., Klein, R. Q. & Saif, M. W. Aurora kinase inhibitors as anti-cancer therapy. *Anti-cancer drugs* **21**, 339–350 (2010).

[97] Marampon, F. *et al.* Close correlation between MEK/ERK and Aurora-B signaling pathways in sustaining tumorigenic potential and radioresistance of gynecological cancer cell lines. *International Journal of Oncology* **44**, 285–294 (2014).

[98] Ruchaud, S., Carmena, M. & Earnshaw, W. C. Chromosomal passengers: conducting cell division. *Nature reviews. Molecular cell biology* **8**, 798–812 (2007).

[99] Rosasco-Nitcher, S. E., Lan, W., Khorasanizadeh, S. & Stukenberg, P. T. Centromeric Aurora-B activation requires TD-60, microtubules, and substrate priming phosphorylation. *Science* **319**, 469–472 (2008).

[100] Song, J., Salek-Ardakani, S., So, T. & Croft, M. The kinases aurora B and mTOR regulate the G1-S cell cycle progression of T lymphocytes. *Nature immunology* **8**, 64–73 (2007).

[101] Nair, J. S. *et al.* Aurora B kinase regulates the postmitotic endoreduplication checkpoint via phosphorylation of the retinoblastoma protein at serine 780. *Mol. Biol. Cell* **20**, 2218–2228 (2009).

[102] Kassardjian, A. *et al.* The transcription factor YY1 is a novel substrate for Aurora B kinase at G2/M transition of the cell cycle. *PLoS ONE* **7**, e50645 (2012).

[103] Terada, Y. Aurora-B/AIM-1 regulates the dynamic behavior of HP1alpha at the G2-M transition. *Mol. Biol. Cell* **17**, 3232–3241 (2006).

[104] Song, K., Jung, Y., Jung, D. & Lee, I. Human Ku70 Interacts with Heterochromatin Protein 1. *Journal of Biological Chemistry* **276**, 8321–8327 (2001).

[105] Yang, C. *et al.* Aurora-B mediated ATM serine 1403 phosphorylation is required for mitotic ATM activation and the spindle checkpoint. *Mol. Cell* **44**, 597–608 (2011).

[106] Hengeveld, R. C. C. *et al.* Development of a chemical genetic approach for human aurora B kinase identifies novel substrates of the chromosomal passenger complex. *Molecular & Cellular Proteomics* **11**, 47–59 (2012).

[107] Gully, C. P. *et al.* Aurora B kinase phosphorylates and instigates degradation of p53. *Proc. Natl. Acad. Sci. U.S.A.* **109**, E1513–1522 (2012).

[108] Wu, L., Ma, C. A., Zhao, Y. & Jain, A. Aurora B interacts with NIR-p53, leading to p53 phosphorylation in its DNA-binding domain and subsequent functional suppression. *J. Biol. Chem.* **286**, 2236–2244 (2011).

[109] Gizatullin, F. *et al.* The Aurora kinase inhibitor VX-680 induces endoreduplication and apoptosis preferentially in cells with compromised p53-dependent postmitotic checkpoint function. *Cancer Research* **66**, 7668–7677 (2006).

[110] Kumari, G., Ulrich, T. & Gaubatz, S. A role for p38 in transcriptional elongation of p21CIP1 in response to Aurora B inhibition. *Cell Cycle* **12**, 2051–2060 (2013).

[111] Trakala, M., Fernández-Miranda, G., De Castro, I. P., Heeschen, C. & Malumbres, M. Aurora B prevents delayed DNA replication and premature mitotic exit by repressing p21Cip1. *Cell Cycle* **12**, 1030–1041 (2013).

[112] Monaco, L. *et al.* Inhibition of Aurora-B kinase activity by poly(ADP-ribosyl)ation in response to DNA damage. *Proceedings of the National Academy of Sciences of the United States of America* **102**, 14244–8 (2005).

[113] Strathdee, C. A., McLeod, M. & Hall, J. Efficient control of tetracycline-responsive gene expression fromm an autoregulated bi-directional expression vector. *Gene* **1**, 21–29 (199).

[114] Gama, V. *et al.* Hdm2 is a ubiquitin ligase of Ku70-Akt promotes cell survival by inhibiting Hdm2-dependent Ku70 destabilization. *Cell Death Differ.* **16**, 758–769 (2009).

[115] Abramoffi, M., Magalh£es, P. & Ram, S. Image proceccing with ImageJ. *Biophotonics International* **11**, 36–42 (2004).

[116] Olive, P. L. & Banáth, J. P. The comet assay: a method to measure DNA damage in individual cells. *Nat. Protoc.* **1**, 23–29 (2006).

[117] Asaithamby, A. & Chen, D. J. Cellular responses to DNA double-strand breaks after low-dose gamma-irradiation. *Nucleic Acids Res.* **37**, 3912–3923 (2009).

[118] Rothkamm, K., Kruger, I., Thompson, L. H. & Lobrich, M. Pathways of DNA double-strand break repair during the mammalian cell cycle. *Mol. Cell. Biol.* **23**, 5706–5715 (2003).

[119] Asaithamby, A. *et al.* Repair of HZE-particle-induced DNA double-strand breaks in normal human fibroblasts. *Radiat. Res.* **169**, 437–446 (2008).

[120] Söderberg, O. *et al.* Direct observation of individual endogenous protein complexes in situ by proximity ligation. *Nature Methods* **3**, 995–1000 (2006).

[121] Gohard, F. H., St-Cyr, D. J., Tyers, M. & Earnshaw, W. C. Targeting the INCENP IN-box-Aurora B interaction to inhibit CPC activity in vivo. *Open Biol* **4**, 140163 (2014).

[122] Bennetzen, M. V. *et al.* Site-specific phosphorylation dynamics of the nuclear proteome during the DNA damage response. *Mol. Cell Proteomics* **9**, 1314–1323 (2010).

[123] Murnion, M. E. *et al.* Chromatin-associated protein phosphatase 1 regulates aurora-B and histone H3 phosphorylation. *J. Biol. Chem.* **276**, 26656–26665 (2001).

[124] Weterings, E. *et al.* A novel small molecule inhibitor of the DNA repair protein Ku70/80. *DNA Repair* **43**, 98–106 (2016).

[125] Alshareeda, A. T. *et al.* Clinicopathological significance of KU70/KU80, a key DNA damage repair protein in breast cancer. *Breast Cancer Research and Treatment* **139**, 301–310 (2013).

[126] Korabiowska, M. *et al.* Differential expression of DNA nonhomologous end-joining proteins Ku70 and Ku80 in melanoma progression. *Mod. Pathol.* **15**, 426–433 (2002).

[127] Korabiowska, M. *et al.* Altered expression of DNA double-strand repair genes Ku70 and Ku80 in carcinomas of the oral cavity. *Anticancer Res.* **26**, 2101–2105 (2006).

[128] Mazzarelli, P. *et al.* DNA end binding activity and Ku70/80 heterodimer expression in human colorectal tumor. *World J. Gastroenterol.* **11**, 6694–6700 (2005).

[129] Forbes, S. A. *et al.* Cosmic: somatic cancer genetics at high-resolution. *Nucleic Acids Research* **45**, D777–D783 (2017).

[130] Roux, K. J., Kim, D. I., Raida, M. & Burke, B. A promiscuous biotin ligase fusion protein identifies proximal and interacting proteins in mammalian cells. *J. Cell Biol.* **196**, 801–810 (2012).

[131] Deng, C. X. BRCA1: cell cycle checkpoint, genetic instability, DNA damage response and cancer evolution. *Nucleic Acids Res.* **34**, 1416–1426 (2006).

[132] d'Adda di Fagagna, F. Living on a break: cellular senescence as a DNA-damage response. *Nat. Rev. Cancer* **8**, 512–522 (2008).

Chapter 6

Appendices

Appendix A

List of Primers

Table A.1: List of Primers, their use, and the 5' to 3' nucleotide sequence.

Primer Name	Use	Sequence
Ku70 N-terminal FW (NdeI)	Ku70 WT-HA pMSCV	GGCCTGCATATGAACCTTGAAG CAAGTGGAGAC
LS Ku HA Rev	Ku70 WT-HA pMSCV	CCACGAATTCTCAAAGAGCGTA ATCTGGAACATCGTATGGGTA CATGTCCTGGAAGT
RV Ku70 Not1	Ku70 pBIG	GGGCTGGCGGCCGCTCAGTCCT GGAAGTGCTTGGT-GAGGGCTT CC
FW Ku70 BamH1 longer	Ku70 pBIG	GGACTAGGATCCATGTCAGGGT GGGAGTCATATTA-CAAAAACGA GGGCG

Appendix B

List of Antibodies

Table B.1: List of antibodies, their relevant dilutions, and source

Antibody	Western Blot Dilution	IF Dilution	Source
HA (H9658)	1:1000	N/A	Sigma-Aldrich
Ku86 (C-20)	1:250	N/A	Santa Cruz
P-Histone H2A.X (S139)(20E3)	N/A	1:1000	Cell Signaling
Ku70 (N3H10)	1:200	1:100	Santa Cruz
Aurora B (ARK-2) (H-75)	1:1000	1:1000	Santa Cruz
T7-tag (D9E1X)(XP)	1:1000	N/A	Cell Signaling
P-Histone H3 (S10)	1:1000	N/A	Cell Signaling
Vinculin (E1E9V)	1:10000	N/A	Cell Signaling

Appendix C

Ku70 S155D and WT expression

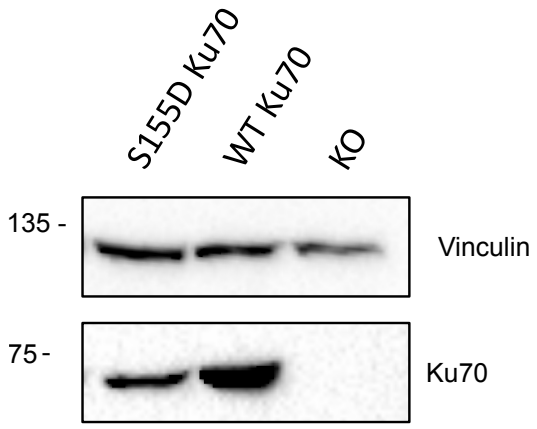

Figure C.1: Ku70 S155D and WT expression following pMSCV infection. pMSCV S155D Ku70, WT Ku70, and empty vector constucts were transfected into phoenix cells which were used to infect Ku70 knockout MEFs. Following puromycin selection of MEFs nuclear extracts were collected and levels of Ku70 in S155D Ku70, WT Ku70, and empty vector infected cells were assessed by western blot. Vinculin was analyzed as a loading control.

Appendix D

Scientific Reports: Publication Rights

Figure D.1: Right to republish data Scientific Reports. As an author of Ku70 Serine 155 mediates Aurora B inhibition and activation of the DNA damage response, I maintain the right to use the data within my thesis.

Chapter 7

Curriculum Vitae

Publications:

Fell, V. L., Walden, E. A., Hoffer, S. M., Rogers, S. R., Aitken, A. S., Salemi, L. M., Schild-Poulter, C. Ku70 Serine 155 mediates Aurora B inhibition and activation of the DNA damage response. Sci. Rep. 6, 37194; doi: 10.1038/srep37194 (2016).

Name:	Elizabeth Walden
Post-Secondary Education and Degrees:	Trent University Peterborough, ON 2010-2014 B.Sc.
	Queens University Kingston, ON 2010-2015 B.Ed.
	University of Western Ontario London, ON 2015 - 2017 M.Sc.
Honours and Awards:	Ontario Graduate Scholarship 2016-2017
	National Science and Engineering Research Council (NSERC) Canada Graduate Scholarship-Masters 2015-2016
	NSERC Undergraduate Student Research Award 2012-2014
	Trent National Renewable Scholarship 2010-2014
	Trent University President's Honour Roll 2010-2014

Related Work Experience:	Teaching Assistant The University of Western Ontario 2015 - 2017
Research Experience	Master of Science Candidate Supervised by Dr. Caroline Schild-Poulter Department of Biochemistry, University of Western Ontario 2015-2017
	Undergraduate Research Project and Summer Student Researcher Supervised by Dr. Yee Trent University 2012-2014